

Spring 5-31-1999

Dual frequency bi-orthogonally polarized antennas for GPS applications

Anand Arun Mahale
New Jersey Institute of Technology

Follow this and additional works at: <https://digitalcommons.njit.edu/theses>



Part of the [Electrical and Electronics Commons](#)

Recommended Citation

Mahale, Anand Arun, "Dual frequency bi-orthogonally polarized antennas for GPS applications" (1999).
Theses. 864.

<https://digitalcommons.njit.edu/theses/864>

This Thesis is brought to you for free and open access by the Electronic Theses and Dissertations at Digital Commons @ NJIT. It has been accepted for inclusion in Theses by an authorized administrator of Digital Commons @ NJIT. For more information, please contact digitalcommons@njit.edu.

Copyright Warning & Restrictions

The copyright law of the United States (Title 17, United States Code) governs the making of photocopies or other reproductions of copyrighted material.

Under certain conditions specified in the law, libraries and archives are authorized to furnish a photocopy or other reproduction. One of these specified conditions is that the photocopy or reproduction is not to be “used for any purpose other than private study, scholarship, or research.” If a user makes a request for, or later uses, a photocopy or reproduction for purposes in excess of “fair use” that user may be liable for copyright infringement,

This institution reserves the right to refuse to accept a copying order if, in its judgment, fulfillment of the order would involve violation of copyright law.

Please Note: The author retains the copyright while the New Jersey Institute of Technology reserves the right to distribute this thesis or dissertation

Printing note: If you do not wish to print this page, then select “Pages from: first page # to: last page #” on the print dialog screen

The Van Houten library has removed some of the personal information and all signatures from the approval page and biographical sketches of theses and dissertations in order to protect the identity of NJIT graduates and faculty.

ABSTRACT

DUAL FREQUENCY BI-ORTHOGONALLY POLARIZED ANTENNA FOR GPS APPLICATIONS

**by
Anand Arun Mahale**

Dual frequency bi-orthogonally polarized antenna to be used in Global Positioning System applications operating in L1 (1575.42 ± 10.23 MHz) and L2 (1227.60 ± 10.23 MHz) Bands has been studied. To ensure compatibility with existing applications, the antenna size is limited in dimensions to 4.120" x 4.680" x 1.250" including the radome. Orthogonally placed two dual frequency probe excited patches were designed using a high dielectric constant substrate ($\epsilon_r = 9.8$ and thickness of 250 mils, Rogers TMM10i material) to obtain vertical and horizontal polarization for each band. The measured performance of this antenna showed good agreement with the specifications required to meet the application needs. As an attractive alternative a stacked dual patch antenna configuration has been suggested and a prototype antenna has also been developed. Using low and high dielectric constants of 2.20 and 9.8 and relative thicknesses of 125 and 250 mils for each layer an orthogonally placed dual patch configuration has been designed, fabricated and tested on a 2 square feet ground plane. Effects of radomes using materials with different permittivities have been studied through numerical simulations and radomes have been fabricated using plastic materials including UMHW, HDPE and Delrin. Numerical simulations have been carried out using IE3D software package developed by Zeland Software Inc. Antennas that were fabricated based on optimized

parameters have further required tuning due to inaccuracies in simulation and material properties. The measurement setup has been enhanced to accommodate axial ratio measurements in polarization pattern characterization by adding a rotary joint to rotate a linearly polarized antenna operating in the receiving mode. The performance characteristics showed that adequate bandwidths and beam widths were obtained and gain of these antennas were measured to be in the order of 3.5 dBi along the main lobe. Further work is continuing to obtain antennas with wider bandwidths using thicker substrates.

**DUAL FREQUENCY BI-ORTHOGONALLY POLARIZED
ANTENNAS FOR GPS APPLICATIONS**

by
Anand Arun Mahale

**A Thesis
Submitted to the Faculty of
New Jersey Institute of Technology
In Partial Fulfillment of the Requirements for the Degree of
Master of Science in Electrical Engineering**

Department of Electrical and Computer Engineering

May 1999

APPROVAL PAGE

DUAL FREQUENCY BI-ORTHOGONALLY POLARIZED ANTENNA

Anand Arun Mahale

Dr. Edip Niver, Thesis Advisor Date
Associate Professor of Electrical and Computer Engineering, NJIT

Dr. Sirin Tekinay, Committee Member Date
Assistant Professor of Electrical and Computer Engineering, NJIT

Dr. Rashid Malik, Committee Member Date
Visiting Professor of Electrical and Computer Engineering, NJIT

Dr. Necdet Uzun, Committee Member Date
Assistant Professor of Electrical and Computer Engineering, NJIT

Dr Lale Alatan, Committee Member Date
Post Doctoral Researcher of Electrical and Computer Engineering, NJIT

BIOGRAPHICAL SKETCH

Author: Anand Arun Mahale

Degree: Master of Science

Date: May 1999

Undergraduate and Graduate Education:

- Master of Science in Electrical Engineering,
New Jersey Institute of Technology, Newark, NJ. 1999
- Bachelor of Science in Electrical Engineering,
Bombay (Mumbai) University, Bombay (Mumbai), India. 1996

Major: Electrical Engineering

To my beloved family, friends and teachers

ACKNOWLEDGEMENT

I would like to express my deepest appreciation to Dr. Edip Niver and Dr. Lale Alatan, who not only served as my research supervisors, providing valuable insight and intuition, but also constantly gave me support, encouragement, and reassurance. I would like to extend my acknowledgements to Mr. Ron Olin and Mr. Mario Casabona of Electro-Radiation Inc. (ERI), Fairfield, NJ, for their guidance and collaboration while sponsoring this project through the funding provided by the grant (Grant No.: 98-2890-020-08) from the New Jersey Commission on Science and Technology. Special thanks are to Mr. Dimple Bhuva, Delta Circuits Inc., and to Mr. Arthur Sutphen, Center for Manufacturing Systems, NJIT, in their help in fabrication of antennas and radomes. Additional thanks are to Mr. Thuan Lam, EM Solutions Inc., for providing software tools and help in simulations. Special thanks are given to Dr. Sirin Tekinay, Dr. Necdet Uzun, and Dr. Rashid Malik for actively participating in my committee.

Many of my fellow graduate students in the Microwave and Lightwave Engineering Laboratory and my friends at New Jersey Institute of Technology deserve recognition for their support.

TABLE OF CONTENTS

Chapter	Page
1. INTRODUCTION	1
1.1 Antennas for Global Positioning System	1
2. MICROSTRIP PATCH ANTENNAS	4
2.1 Introduction	4
2.2 Microstrip Resonator Classification	4
2.3 Analytical Modes For Rectangular Patch Antenna	6
2.4 Transmission Line Model	7
2.5 Cavity Model	14
2.6 Microstrip Antenna Feeds	17
2.7 CAD Design and Analysis of a Rectangular Microstrip Patch Antenna	18
3 DUAL FREQUENCY BI-ORTHOGONALLY POLARIZED MICROSTRIP ANTENNA	24
3.1 Introduction	24
3.2 GPS Antenna Requirements	24
3.3 Dual Frequency Antennas	28
4 EXPERIMENTAL RESULTS AND DISCUSSIONS	36
4.1 Coplanar, Orthogonal Rectangular Dual Patch Antenna	36
4.2 Stacked Orthogonally Polarized Rectangular Patch Antennas	45
5 CONCLUSIONS	54
APPENDIX ELECTROMAGNETIC SIMULATION SOFTWARE	56
REFERENCES	60

LIST OF TABLES

Table	Page
4.1 Radiation Efficiency Versus ϵ_r of the Radome for a Single Patch of $\epsilon_r = 10$ and thickness $t = 250$ mils	39

LIST OF FIGURES

Figure	Page
1.1 Dual Frequency Patch Antenna	3
2.1 Various Microstrip Patch Antennas	5
2.2 Microstrip Antenna and its Equivalent Transmission Line Model	9
2.3 Microstrip Line and Effective Dielectric Constant	10
2.4 Physical and Effective Length of a Rectangular Microstrip Patch	13
2.5 Rectangular Microstrip Patch Geometry for a Cavity Model	15
2.6 Field Configurations (modes) for a Rectangular Microstrip Patch	16
2.7 Probe Fed Structure of the Antennas Developed for GPS Applications	19
2.8 Current Distribution of a Rectangular Patch Antenna	20
2.9 Current Distribution of a Stacked Patch Antenna	21
3.1 Specified Dimensions of the GPS Antenna	25
3.2 Orthogonal Mode Dual Frequency Patch Antenna	29
3.3 Multipatch Dual Frequency Antenna	30
3.4 Bi-orthogonally Polarized Dual Frequency Stacked Patch Antenna	31
3.5 Reactively Loaded Antennas	33
3.6 Aperture E-Field Distribution of TM_{10} and TM_{30} modes	34
3.7 Aperture H-Field Distribution of TM_{10} and TM_{30} modes	35
4.1 Co-planar Orthogonal Rectangular Patches	37
4.2 Simulation Results of the Input Return Loss of the Co-planar Antenna	38
4.3 Measured Input Return Loss Graph for Port 1 and Port 2	41

**LIST OF FIGURES
(Continued)**

Figure	Page
4.4 Measured Input Return Loss Graph for Port 3 and Port 4	42
4.5 Radiation Patterns at 1.227 GHz for Vertical Polarization	43
4.6 Radiation Patterns at 1.227 GHz for Horizontal Polarization	43
4.7 Radiation Patterns at 1.575 GHz for Vertical Polarization	44
4.8 Radiation Patterns at 1.575 GHz for Horizontal Polarization	44
4.9 Stacked Orthogonal Rectangular Patch Antennas	45
4.10 Simulation Results for the Input Return Loss of the Stacked Antenna	47
4.11 Measured Input Return Loss Graphs for Port 1 and Port 2	48
4.12 Radiation Patterns at 1.227 GHz for Vertical Polarization	49
4.13 Radiation Patterns at 1.227 GHz for Horizontal Polarization	50
4.14 Radiation Patterns at 1.575 GHz for Vertical Polarization	50
4.15 Radiation Patterns at 1.575 GHz for Horizontal Polarization	51
4.16 Polarization Patterns of the Stacked Antenna Connected to a Hybrid Coupler at 1.575 GHz	53

CHAPTER 1

INTRODUCTION

1.1 Antenna For Global Positioning System

Dual frequency bi-orthogonally polarized antenna for use in Global Positioning System (GPS) receivers operating at L1 (1.57542 GHz) and L2 (1.22760 GHz) frequency bands were studied. The primary objective of this effort is to develop GPS antenna configurations that are suitable for use with new signal processing techniques being developed by Electro-Radiation Incorporated (ERI), Fairfield, NJ [1]. The parameters such as antenna gain, efficiency, radiation characteristics and bandwidth of the developed antenna are very critical for successful GPS reception in terms of increasing the antenna signal to noise performance. By packaging this antenna configuration into a compact patch type structure it will be suitable for use on the wide variety and large number of military and commercial vehicles such as aircrafts, helicopters, tanks, missile launchers, ships and automobiles which use GPS receivers for navigation purposes.

Microstrip antennas [2] have found use in diverse applications due to their light weight, compact size, rugged and conformal characteristics and often lower costs in materials and mass production. Although the dual frequency dual polarization antenna elements have been reported before [2], the GPS application oriented antenna proposed in this work has its unique characteristics. The parameters that dictate the antenna requirements, for current GPS system applications require dual frequency reception in L1 and L2 bands with orthogonal polarization. Research on dual frequency patch

antennas that have been carried out in the last decade has been summarized in a recent publication [3], indicating that dual frequency antennas can be grouped accordingly, as shown in

Figure 1,

- Orthogonal dual frequency patch antenna,
- Multipatch dual frequency patch antenna,
- Reactively loaded patch antenna.

However, the current requirement also seeks dual orthogonal polarization for both L1 and L2 frequency bands. The proposed solution in this work includes combination of

- Two orthogonal mode dual frequencies patch antennas,
- Two orthogonal dual frequency stacked patch antennas.

The above combined antenna structures were designed based on numerical simulations, fabricated and tested.

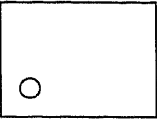
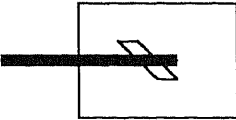
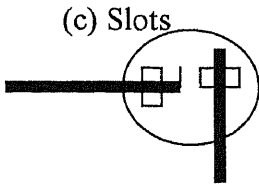
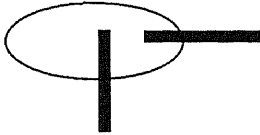
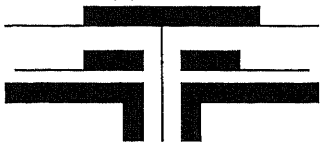
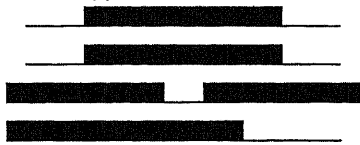
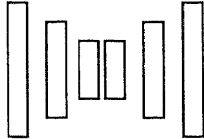
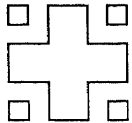

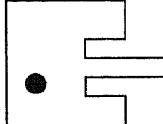
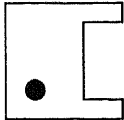
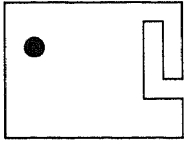
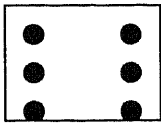
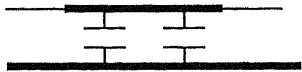
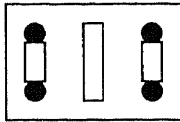
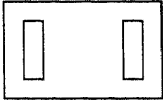
Orthogonal Modes	
<i>Single-Point</i>	<div style="display: flex; justify-content: space-around;"> <div style="text-align: center;"> <p>(a) Probe</p>  </div> <div style="text-align: center;"> <p>(b) Slot</p>  </div> </div>
Dual-Point	<div style="display: flex; justify-content: space-around;"> <div style="text-align: center;"> <p>(c) Slots</p>  </div> <div style="text-align: center;"> <p>(d) EMC</p>  </div> </div>
Multi-Patch	
Stacked	<div style="display: flex; justify-content: space-around;"> <div style="text-align: center;"> <p>(e) Probe</p>  </div> <div style="text-align: center;"> <p>(f) Slot</p>  </div> </div>
Co-Planar	<div style="display: flex; justify-content: space-around;"> <div style="text-align: center;"> <p>(g) Dipole</p>  </div> <div style="text-align: center;"> <p>(h) Cross-subarray</p>  </div> </div>
Reactively Loaded	
Stubs	<div style="display: flex; justify-content: space-around;"> <div style="text-align: center;"> <p>(i) Coaxial</p>  </div> <div style="text-align: center;"> <p>(j) microstrip</p>  </div> </div>
Noches	<div style="display: flex; justify-content: space-around;"> <div style="text-align: center;"> <p>(k) Inset</p>  </div> <div style="text-align: center;"> <p>(l) Spur-line</p>  </div> </div>
Pins and Capacitors	<div style="display: flex; justify-content: space-around;"> <div style="text-align: center;"> <p>(m) Pins</p>  </div> <div style="text-align: center;"> <p>(n) Capacitors</p>  </div> </div>
Slots	<div style="display: flex; justify-content: space-around;"> <div style="text-align: center;"> <p>(o) Slots and Pins</p>  </div> <div style="text-align: center;"> <p>(p) Slots</p>  </div> </div>

Figure 1.1. Dual Frequency Patch Antennas

CHAPTER 2

MICROSTRIP PATCH ANTENNAS

2.1 Introduction

Low profile, light weight, ease in fabrication, rugged, conformal, and in some cases lower cost than comparable antennas, are among favorable features which help microstrip antenna to be used in a broad range of modern applications. Microstrip antennas have been designed and incorporated in very wide range of systems, from commercial car navigation GPS systems, biomedical systems, intruder alarms, to sophisticated satellite communication systems, on board ship radar, aircraft antennas, etc. They are especially suitable for low power and narrow bandwidth applications due to their inherent limitations of handling high power and delivering wide bandwidths. Furthermore, the inherent limited polarization purity can be improved by choosing configurations, which combine orthogonal polarizations.

2.2 Microstrip Resonator Classification

The basic microstrip resonator [4] geometry given in Figure 2.1 consists of a dielectric sheet of thickness h and relative dielectric constant ϵ_r . The finite conductor with a variety of shapes is deposited on the top of the dielectric helps the entire resonating structure to radiate. The microstrip radiator can be classified in two categories; the narrow strip resonator is usually called the microstrip dipole antenna whereas the broader

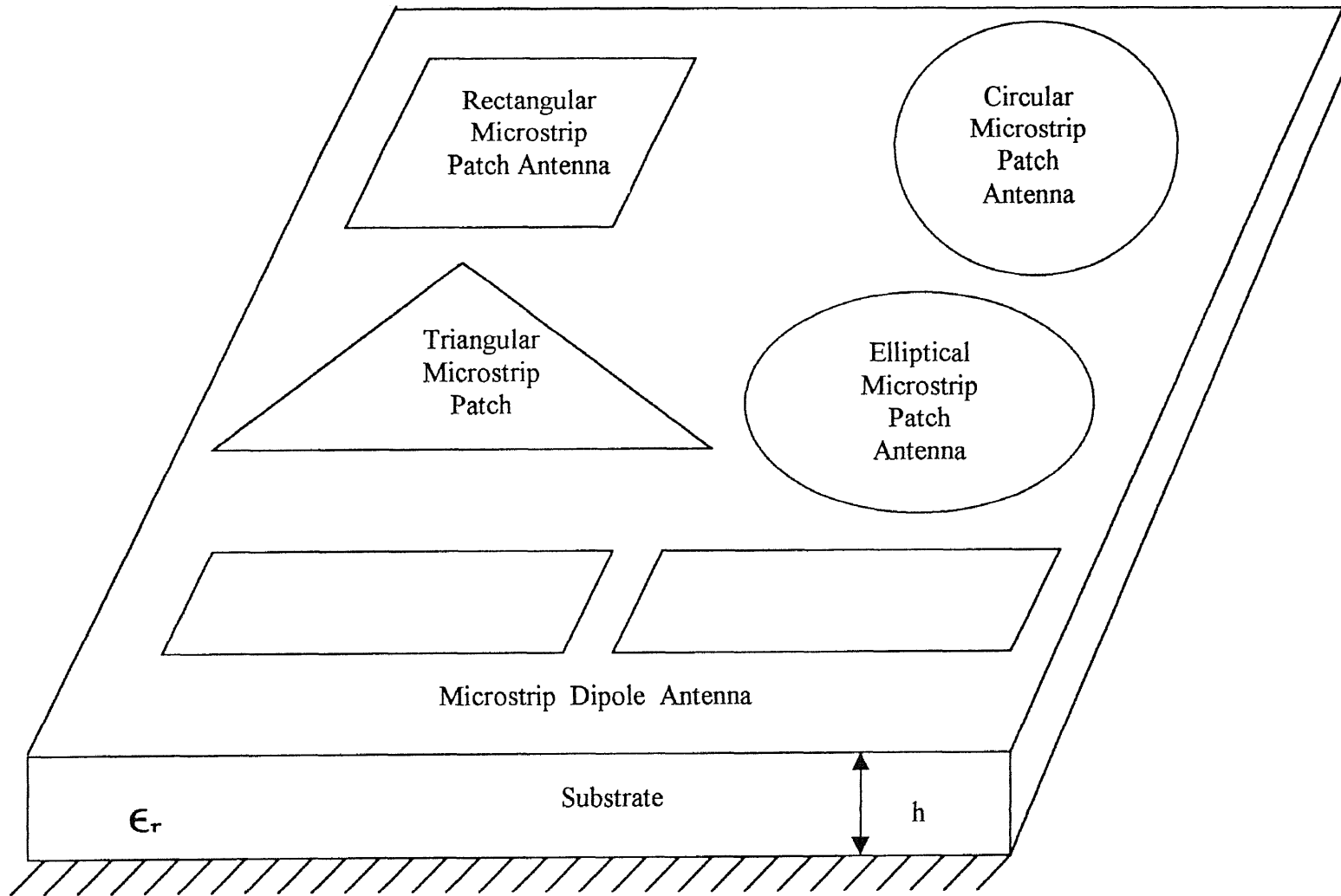


Figure 2.1. Various microstrip patch antennas.

conductor is known as a microstrip patch antenna. Figure 2.1 illustrates various shapes of microstrip patch antennas and a dipole microstrip antenna. Microstrip patch antenna may have varieties of shapes: rectangular, square, circular, ring, triangular, or elliptical as shown in Figure 2.1. The selection of a particular shape depends on the parameters one wishes to optimize: e.g. antenna size, sidelobe levels, cross polarization factors, impedance bandwidth, etc. Because of the broader width, a microstrip patch antenna may excite surface current flowing across the transverse direction which will in turn create unwanted cross polarization radiation interference effects. The intensity of this undesired radiation depends strongly on the feeding methods and location of the feed and primarily on the thickness of the substrate in terms of a free space wavelength.

2.3 Analytical Modes for Rectangular Patch Antennas

Although the geometry of a rectangular microstrip antenna appears to be simple, it becomes quite difficult to determine the electromagnetic field effects analytically due to the presence of complex boundary conditions at the interface between dielectric substrate, metal, and air. For more accurate analysis, a full-wave electromagnetic solver is employed based on methods of numerical solution of Maxwell's equations. Brief outline of the currently used numerical methods is given in Appendix A. In this work, as an example, software package IE3D (Integration Equation Solution 3D) developed by Zealand Software Inc., is used to analyze and design a dual frequency dual patch microstrip antenna operating at L1 and L2 bands.

Even though, one can obtain accurate results for patch radiation using software tools, simulations alone may not be able to lead to simple interpretations on how radiation takes place. Simple approximate analytical models help to fill in such gaps. The

common analytical models are based on an equivalent transmission line model and a cavity model. A combination of both simplified models and accurate numerical analysis results will offer better insight on how such a structure radiates.

2.4 Transmission Line Model

A transmission line model [5] is the simplest of all approximate methods. It utilizes transmission line theory to model the patch in terms of parallel radiating slots as shown in Figure 2.2. Each radiating slot has a length 'w' and width proportional to height 'h'. Because of its simplicity, it provides results with limited accuracy; however, it does suggest some physical insights on how energy radiates into upper half space. But it does not predict the presence of higher order modes. The more complicated cavity model can predict the existence of higher modes, however it does not lead to equivalent sources that result in radiation.

A. Microstrip transmission line

A microstrip line consists of a strip conductor and a ground plane separated by a dielectric substrate as shown in Figure 2.3. Both electric and magnetic fields are not confined entirely within the substrate below the conducting patch but partial fringing fields also exist in air so the propagation of electromagnetic energy in the microstrip line is not restricted to a pure transverse electromagnetic (TEM) mode but necessitates inclusion of a quasi-TEM mode as well. The characteristic impedance of the microstrip line can be expressed as [6]

$$Z_0 = \frac{60}{\sqrt{\epsilon_{r,\text{eff}}}} \ln \left[\frac{8}{w/h} + 0.25(w/h) \right] \quad \text{for } (w/h) \leq 1 \quad (2.1)$$

Where $\epsilon_{r,\text{eff}}$ denotes the effective dielectric constant, which will be defined in the following section.

$$Z_0 = \frac{(120 / \sqrt{\epsilon_{r,\text{eff}}})}{\left(\frac{w}{h} + 1.393 + 0.667 \ln \left(\frac{w}{h} + 1.444 \right) \right)} \quad \text{for } (w/h) \geq 1 \quad (2.2)$$

B. Effective dielectric constant

With finite line width, the fields at the edge undergo fringing and make the microstrip line appear wider electrically compared to its actual physical dimensions. Effective dielectric $\epsilon_{r,\text{eff}}$ is introduced to account for both fringing and the presence of a quasi-TEM mode. Effective relative dielectric constant is defined as the relative dielectric constant of the corresponding uniform dielectric material so that the electrical characteristics of the structure in Figure 2.3(b) are the same as in Figure 2.3(c) especially in terms of the propagation constant. The effective dielectric constant of a microstrip line is a function of the dielectric constant ϵ_r , the height h of the dielectric substrate, and the width w of the strip conductor, which is given by [7]:

If $t/h \ll 0.005$:

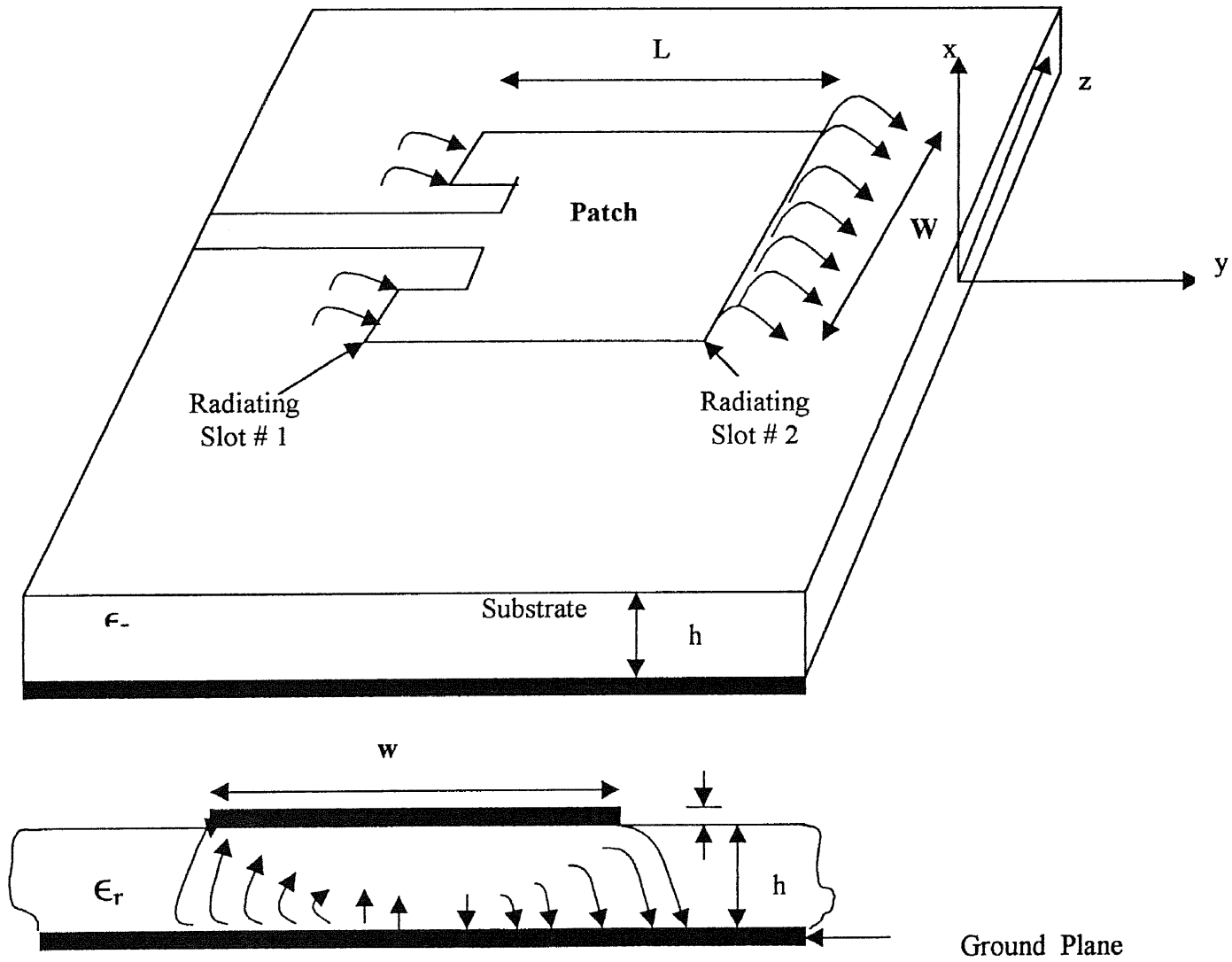
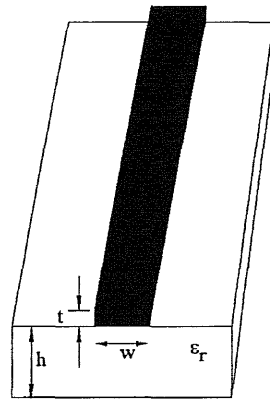
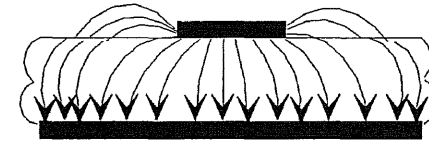


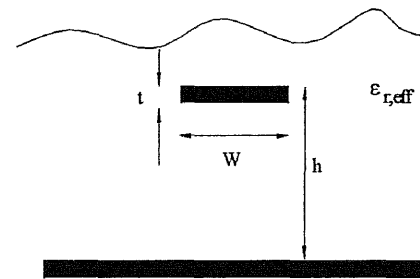
Figure 2.2. Microstrip Antenna and its Equivalent Transmission Line Model



Microstrip line



Electric fields and fringing fields



Effective dielectric constant

Figure 2.3. Microstrip line and effective dielectric constant

$$\epsilon_{r,\text{eff}} = \frac{(\epsilon_r + 1)}{2} + \frac{(\epsilon_r - 1)}{2} \left[\left(\frac{1 + 12}{(w/h)} \right)^{-1/2} + 0.04 \left(1 + \frac{w}{h} \right)^2 \right] \text{ for } (w/h) \leq 1$$

$$\epsilon_{r,\text{eff}} = \frac{(\epsilon_r + 1)}{2} + \frac{(\epsilon_r - 1)}{2} \left[1 + \frac{12}{(w/h)} \right]^{-1/2} \text{ for } (w/h) \geq 1 \quad (2.3)$$

C. Effective length, effective width, and resonant frequency

Because of the fringing field effects on the radiating edge of the microstrip patch antenna, its effective length will be longer than its physical dimension as shown in Figure 2.4. Its length is extended by an additional amount of Δl on both ends of the radiating edge and expressed as [8]

$$\frac{\Delta L}{h} = 0.412 \left(\frac{\epsilon_{r,\text{eff}} + 0.3}{\epsilon_{r,\text{eff}} - 0.258} \right) \left[\frac{(w/h) + 0.264}{(w/h) + 0.8} \right] \quad (2.4)$$

Since additional length $2\Delta l$ added into the total length L , the effective length of this patch will be $L_{\text{eff}} = L + 2\Delta l$.

The resonant frequency of the patch antenna is given by

$$f_{r,\text{eff}} = \frac{1}{2L \left(\sqrt{\epsilon_{r,\text{eff}}} \sqrt{\mu_0 \epsilon_0} \right)} = \frac{c}{2L \sqrt{\epsilon_r}} \quad (2.5)$$

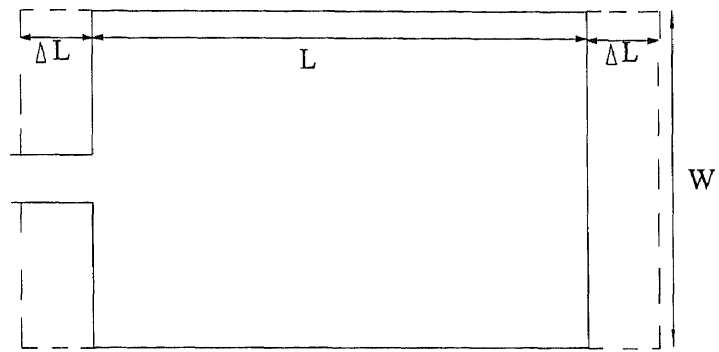
where c is the velocity of light in vacuum. Above formula did not take into account the modified value of the effective length. Therefore, a more accurate version of resonant frequency for the patch can be expressed as [4]:

$$\begin{aligned}
 f_{r,\text{eff}} &= \left[q \left(\frac{1}{2 L_{\text{eff}} \sqrt{\epsilon_{r,\text{eff}}} \sqrt{\mu_0 \epsilon_0}} \right) \right] \\
 &= q \left(\frac{c}{2 L_{\text{eff}} \sqrt{\epsilon_{r,\text{eff}}}} \right) = q f_r \quad (2.6)
 \end{aligned}$$

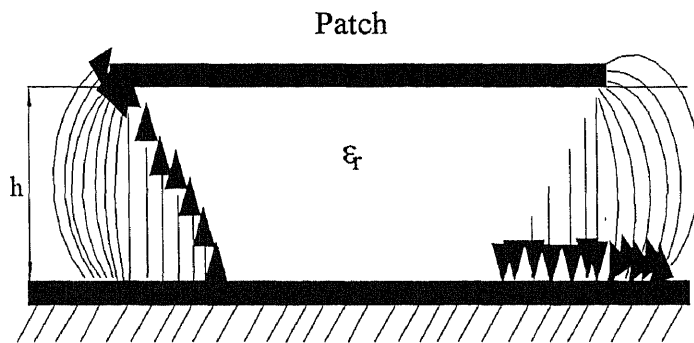
$$q = \frac{f_{r,\text{eff}}}{f_r} \quad (2.7)$$

where q is defined as the fringing factor or length reduction factor.

From transmission line model, one can estimate the resonant frequency of the rectangular microstrip patch antenna. When the substrate height increases, extended fringing causes Δl to expand which forces the decrease in the resonant frequency, but may lead to excitation of surface waves [9].



(a) Top view



(b) Side view

Figure 2.4. Physical and effective length of rectangular microstrip antenna

2.5 Cavity Model

Cavity model is more complex in nature in comparison to the transmission line model.

Here, the rectangular microstrip patch is modeled as a dielectric loaded cavity where the normalized field within the dielectric substrate can be calculated accurately by assuming that region as a cavity bounded by the patch and the bottom ground plane (perfect conducting electric walls) with perfect conducting magnetic walls in surrounding perimeter of the patch as shown in Figure 2.5. Cavity model has the ability to predict higher order modes supported by the structure and the corresponding resonant frequencies for the cavity are given as [10, 11]:

$$(f_{r,eff})_{mnp} = \frac{1}{2\sqrt{\mu\epsilon}} \sqrt{\left(\frac{m}{h}\right)^2 + \left(\frac{n}{L}\right)^2 + \left(\frac{p}{W}\right)^2} \quad (2.8)$$

where m , n , p represent the number of half-cycle field variations along the x , y , z directions, respectively. As the dielectric substrate is thin no field variation with respect to ' x ' is assumed. Hence ' $m = 0$ '. Therefore the two dominant modes that would be excited orthogonally are TM_{01} and TM_{10} modes. Figure 2.6 shows the field configurations for the dominant and the first three higher order modes.

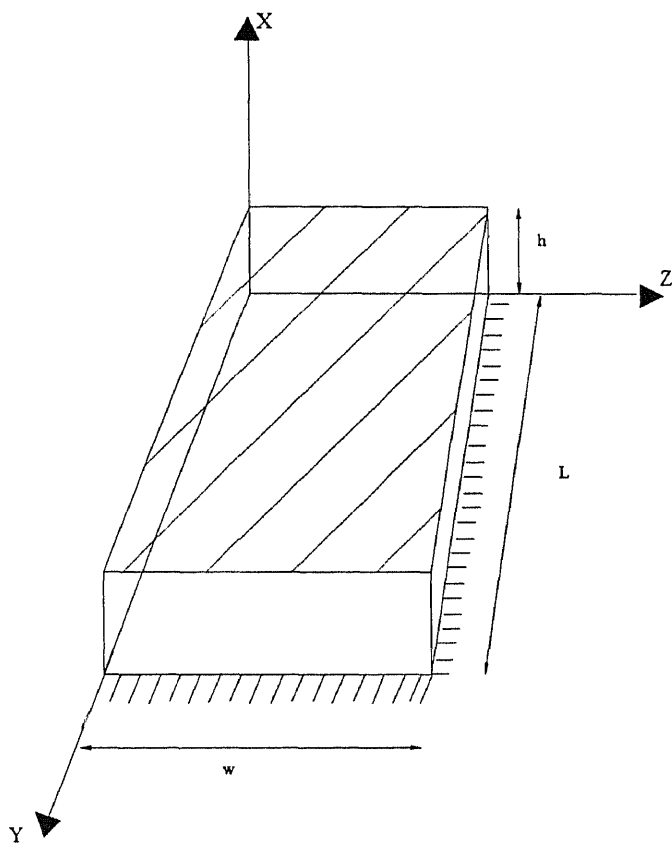


Figure 2.5. Rectangular microstrip patch geometry for a cavity model [8].

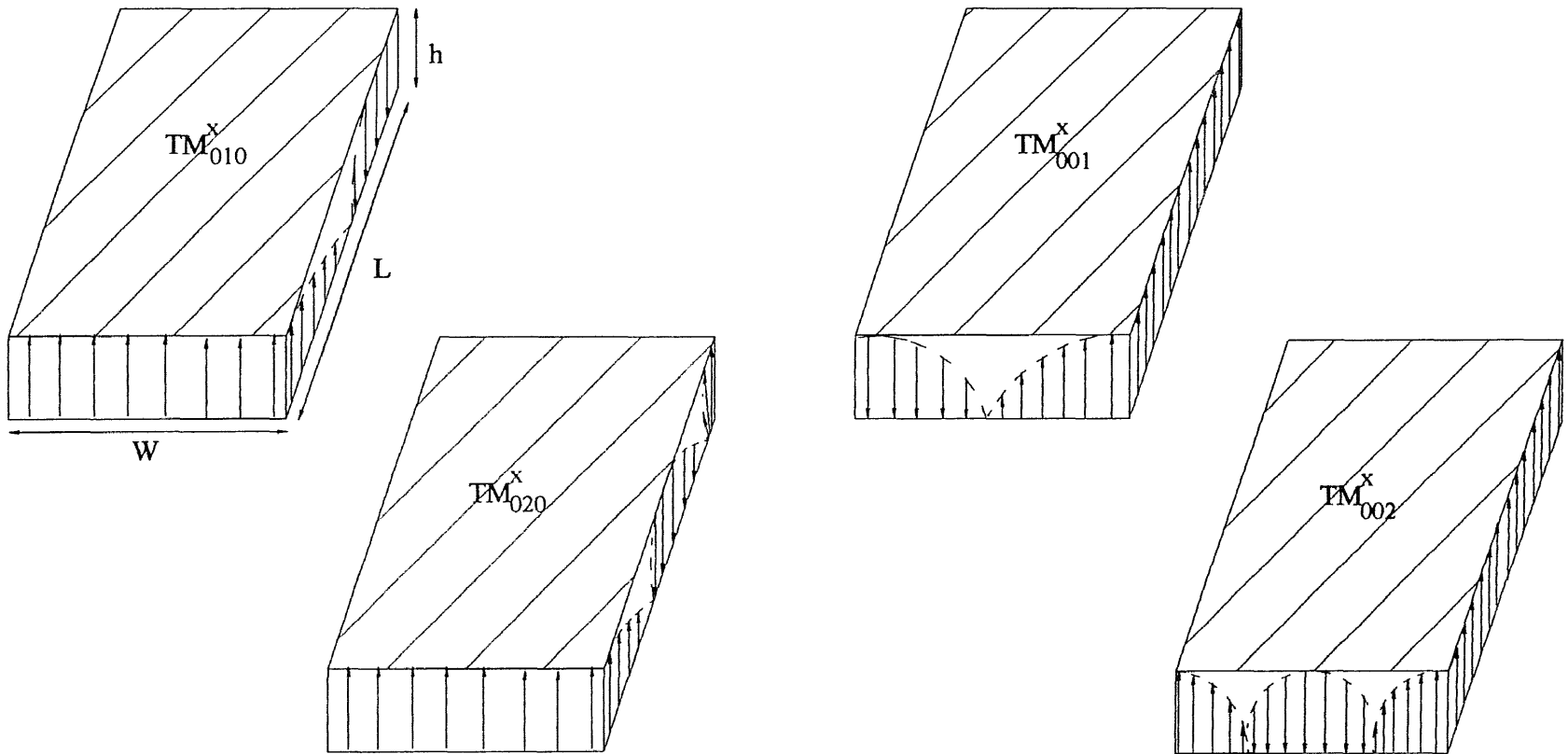


Figure 2.6. Field configurations (modes) for a rectangular microstrip antenna

A. Radiation patterns of a rectangular microstrip patch antenna

The approximate far field radiation patterns of a rectangular microstrip antenna operating in the dominant mode in both E and H planes, respectively are given by [4]:

E – Plane :

$$E_{\phi} = -j \frac{2 k_0 w V_0 e^{-jk_0 r}}{\pi r} \left[\frac{\text{Sin}((k_0 h / 2) \text{Cos}\phi)}{(k_0 h / 2) \text{Cos}\phi} \right] \text{Cos}((k_0 L_{\text{eff}} / 2) \text{Sin}\phi) \quad (2.9)$$

H – Plane :

$$E_{\phi} = -j \frac{2 k_0 w V_0 e^{-jk_0 r}}{\pi r} \text{Sin}\theta \left[\frac{\text{Sin}((k_0 h / 2) \text{Sin}\theta) \text{Sin}(k_0 w / 2) \text{Cos}\theta}{(k_0 h / 2) \text{Sin}\theta (k_0 w / 2) \text{Cos}\theta} \right] \quad (2.10)$$

Where, $V_0 = hE_0$, is the voltage across the slot,

$E_0 = -j \omega A_{mnp}$, is the amplitude of the electric field,

A_{mnp} = represents the amplitude coefficients of each ‘mnp’ mode.

k_0 = wavenumber.

2.6 Microstrip Antenna Feeds

Coaxial feed (probe feed), direct microstrip (inset and non-radiating) feed, proximity feed, and aperture coupled feed could be considered among the most popular feed structures utilized in excitation of microstrip antennas [9].

Coaxial feed is widely used as a microstrip feed due to its ease in fabrication. The probe extends from underneath the ground plane, penetrates through the substrate, and is connected to the patch. It is totally hidden under the big patch therefore theoretically

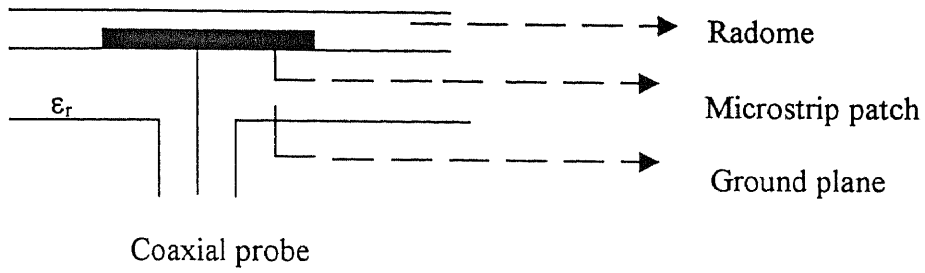
generates no spurious radiation. In this work probe feed is used partially for single layer patch antenna excitation and aperture coupled feed is used for stacked antenna as shown in Figure 2.7. IE3D simulations yielded the graphical representation of the vector current distribution due to coaxial feed and aperture coupled feed used in this work for single layer and stacked antenna respectively. These distributions are shown in the Figure 2.8 and 2.9.

2.7 CAD Design and Analysis of a Rectangular Microstrip Patch Antenna

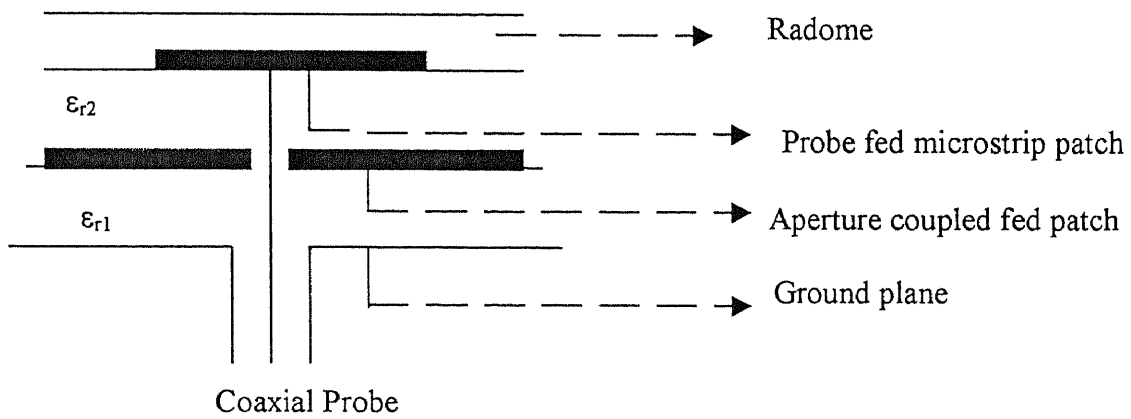
In order to facilitate the design process, with the help of simplified models, initial values for resonant frequency and the feed location can be estimated. Approximate results provide good initial values for further optimization in numerical simulations. The pre-calculated dimensions and the feed point location are entered through MGRID, which is a Windows 95 graphical interface circuit layout editor of IE3D package. The first run simulated results are analyzed to identify where resonant frequency shift is and also helps to determine the nature of the impedance of the antenna at the chosen feed location.

A.) Resonant frequency of the patch

The resonant frequency is determined through the zero cross over of the imaginary part of the impedance. The desired requirement necessitates that for maximum radiation, the antenna impedance should be purely resistive and the radiation resistance should be equal to the generator's impedance to ensure maximum power transfer. If there is cancellation of reactive components in terms of either capacitive or inductive reactance, the net energy

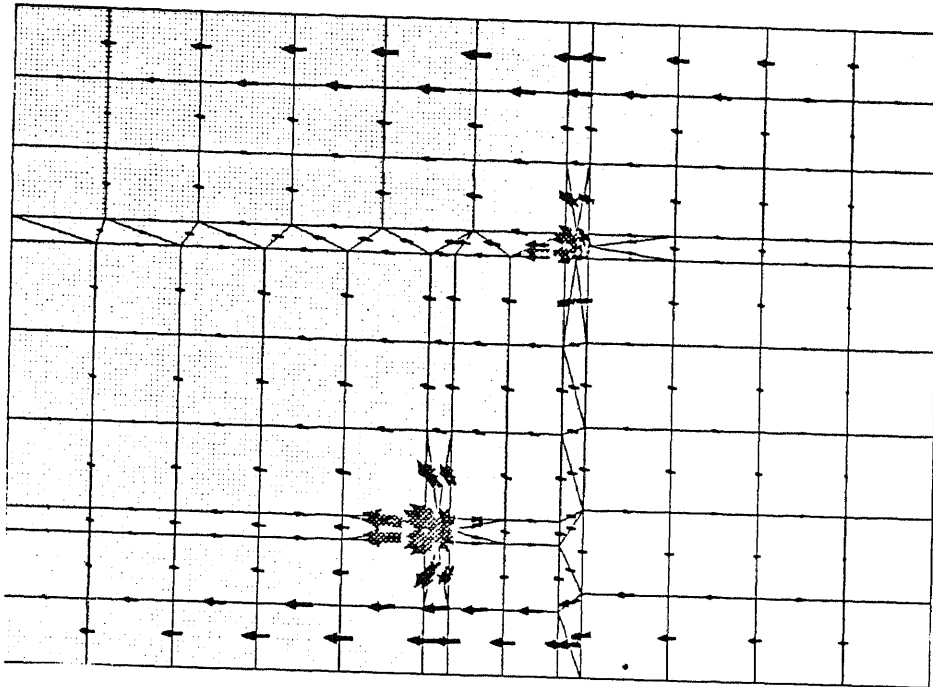


(a) Probe fed patch antenna

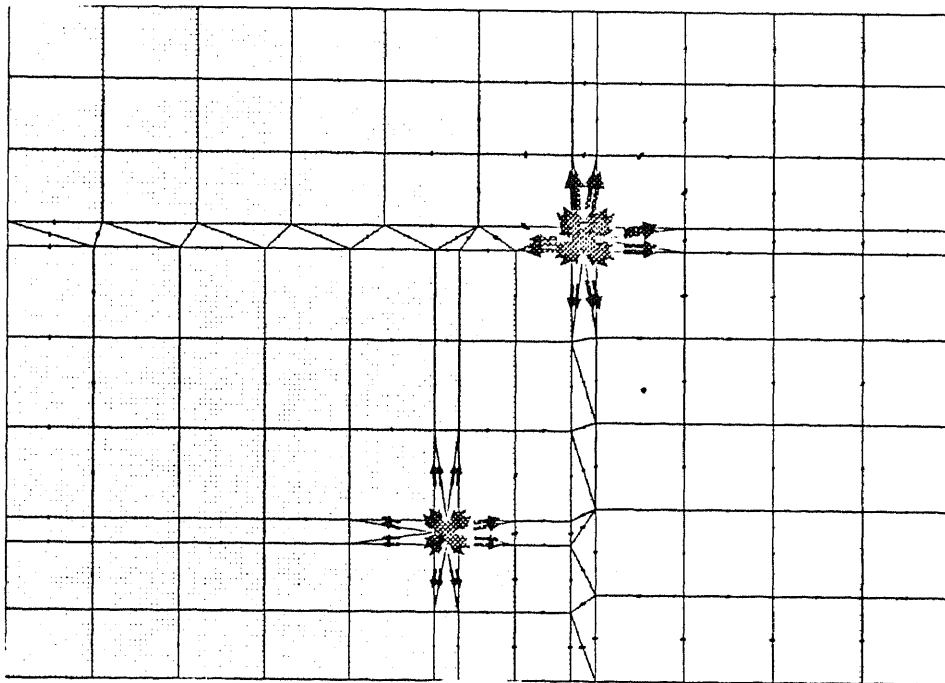


(b) Probe and aperture coupled fed stacked antenna

Figure 2.7. Probe feed structures of the antennas developed for GPS applications.

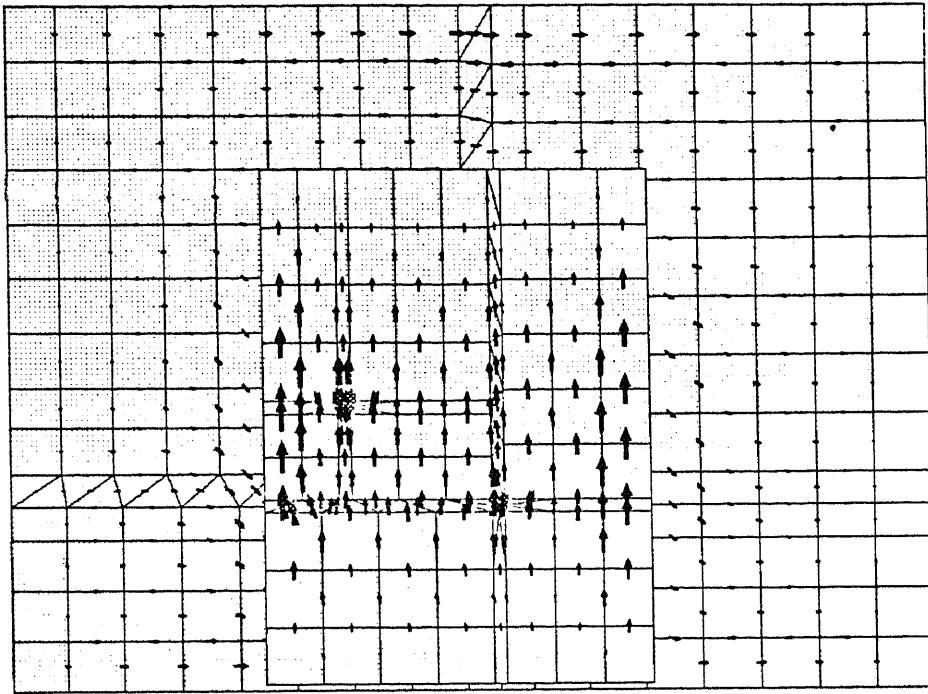


(a) Frequency = 1.227 GHz

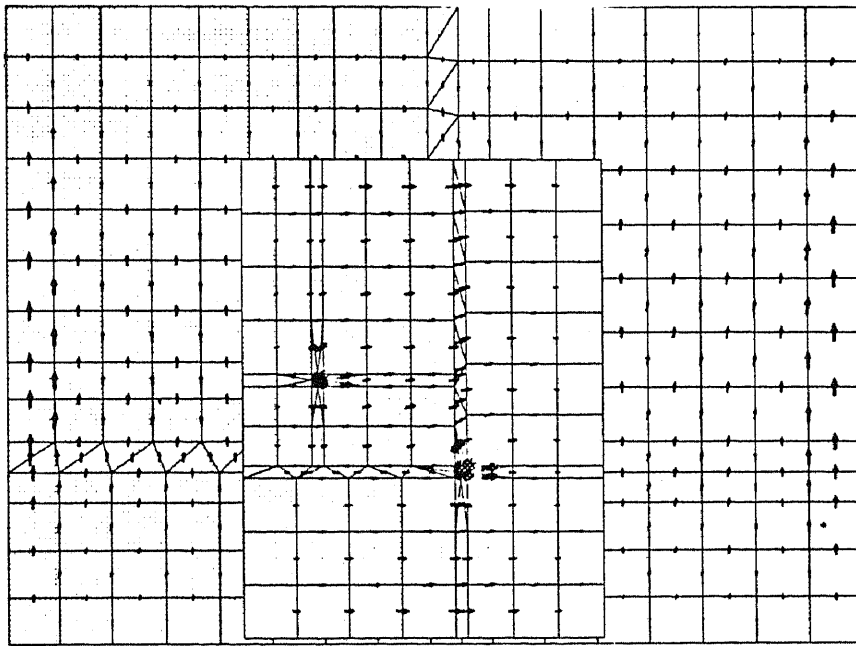


(b) Frequency = 1.575 GHz

Figure 2.8. Current distribution of a rectangular patch antenna



(a) Frequency = 1.227 GHz



(b) Frequency = 1.575 GHz

Figure 2.9. Current distribution of a stacked patch antenna

storage will not take place and all resistive power left after experiencing possible losses will radiate.

B. Determination of the matched feed location

The proper feed location is determined by observing the impedance of the antenna at the resonant frequency. Figure 2.8 and 2.9 show the current density distribution of the patch. One can easily observe that the current is minimum at the edge and maximum in the middle of the non-radiating edge, therefore the impedance is minimum at the center and maximum at the edge. With this information one can immediately predict whether the feed location should be moved forward or backward, accordingly.

C. Optimization for the resonant frequency and the matched feed

When the probe is moved to a new location, the resonant frequency will be affected due to the interaction of the impedance of the probe with the patch. Adjusting the length of the patch for changing resonant frequency also changes the impedance of the antenna. The total length adjustment leads to the changes in a current density distribution at that location, resulting in modification of the impedance of the antenna.

Most optimization schemes are based on a linear optimization requiring the user to define the solution of the problem as close to the optimum as possible, otherwise iterative solution may be locked into to the local minimum, preventing the proper convergence for the final solution. As in the case of the patch antenna analyzed here, the user must be able to tune the antenna to the closest possible length and identify the proper feed location. Then, these solutions should be placed into the geometry file for final

optimization. The obtained optimized results were quite impressive, most of the time very good return loss can be achieved somewhere between -50 to -60 dB for a single patch antenna as seen in Figure 4.2. This result could be hardly obtained without the help of the built-in optimization routine in IE3D.

Although the cavity model predicts the presence of higher order modes, the resonance frequencies corresponding to these modes are not of any practical interest in this work, since L1 band (1.57542 GHz) is below the second harmonic of the L2 band (1.22760 GHz).

CHAPTER 3

DUAL FREQUENCY BI-ORTHOGONALLY POLARIZED MICROSTRIP ANTENNA

3.1 Introduction

Most applications that require dual frequency operation may require wider bandwidth than the one that can be obtained by a single microstrip antenna. Some dual frequency systems operate on the transmit-receive bands whereas other applications such as Global Positioning System (GPS) require two distinct bands for accuracy enhancement. The goal of this effort is to design and build a prototype dual frequency (L1 and L2 bands) antenna having two orthogonal polarizations (Vertical and Horizontal) or (Right Hand Circular Polarization (RHCP) and Left Hand Circular Polarization (LHCP)).

3.2 GPS Antenna Requirements

One of the main factors is the size requirement for numerous GPS applications, i.e. in this particular case the physical dimensions should not exceed 4.120" x 4.680" x 1.25", including the radome. Figure 3.1, depicts the required physical dimensions which are consistent with the existing installations would be adhered in this work. The typical attribute of the microstrip antenna is its narrow bandwidth. However wider bandwidth requirement can be met to a certain extent by changing the substrate thickness or modifying the patch geometry.

The current desired specifications for the dual frequency bi-orthogonally polarized antenna are:

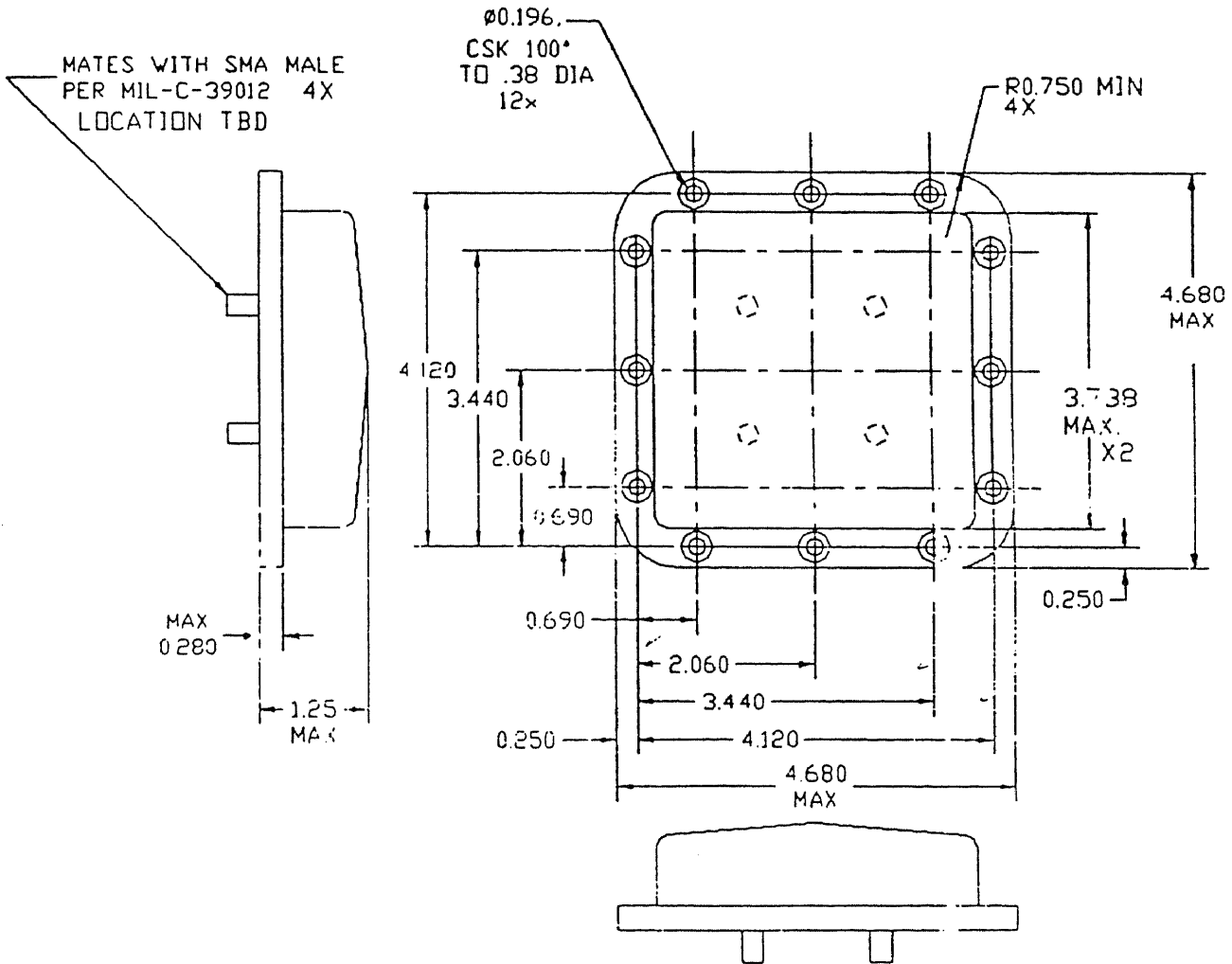


Figure 3.1. Specified dimensions of the GPS antenna.

- **Item Definition:** The dual frequency bi-orthogonally polarized antenna will include the antenna elements, radomes, mechanical interface and electrical connectors.
- **Interface Definition:** The dual frequency bi-orthogonally polarized antenna shall have an outline and mechanical configuration in accordance with Figure 3.1.
- **Characteristics:**
 - RF Frequency:** The dual frequency bi-orthogonally polarized antenna shall meet its performance requirements for the following frequencies:
RF1: 1575.42 ± 10.23 MHz
RF2: 1227.60 ± 10.23 MHz
 - Polarization:** Dual Orthogonal Linear polarization shall be provided for each RF frequency specified in the above paragraph.
 - Mounting Location:** The dual frequency bi-orthogonally polarized antenna is intended as a top mounted antenna installation.
 - Antenna Gain:** The dual frequency bi-orthogonally polarized antenna shall provide a minimum gain of 0 dBi over a 160 degree solid angle cone of coverage (above 10 degree elevation angle) for matched polarization signals within the RF1 and RF2 bandwidths these gain requirements shall be met using a test ground plane two feet square.
 - VSWR:** The dual frequency bi-orthogonally polarized antenna VSWR at the signal interface shall not exceed 1.8: 1 referenced to 50-ohm characteristic impedance over the RF1 and the RF2 bandwidths.

Power Consumption: The dual frequency bi-orthogonally polarized antenna shall be passive and require no electrical power.

Environmental Conditions: The antenna unit is intended for outdoor applications in both ground based and air borne installations and shall withstand such environment without sustaining damage or degraded performance.

Temperature: The dual frequency bi-orthogonally polarized antenna shall be designed to operate at the temperature range -54°C to $+71^{\circ}\text{C}$ with storage to $+95^{\circ}\text{C}$.

Altitude and Humidity: The unit shall withstand altitude of -1500 to $70,000$ feet, and relative humidity upto 100% , including conditions where condensation takes place.

- **Design and Construction:** The unit shall be designed for outdoor ground and airborne applications and shall use applicable portions of MIL-E-5400 and MIL-E-16400 as a guide.

- **Testing**

First Article Tests: E&H plane patterns shall be taken for RF1 and RF2 for each associated port. Calibration of absolute gain at boresight shall be obtained for each frequency. All data shall be taken while dual frequency bi-orthogonally polarized antenna is mounted to a 2 feet square ground plane.

3.3 Dual Frequency Antennas

Dual frequency antennas consist of a single radiating structure, which exhibits a resonant behavior, both in terms of radiation and impedance matching at two separate frequencies. In microstrip antenna technology, dual frequency operation can be achieved through several numbers of different configurations. The basic three categories are [3],

1. Orthogonal Mode Dual Frequency Patch Antenna,
2. Multipatch Dual Frequency Antenna,
3. Reactively Loaded Patch Antenna.

Radiation efficiency, input impedance matching, dual frequency ratio, ease of fabrication and cost are the primary factors that effect the choice of an optimum configuration suitable for a specific application. Hence performance of each category will be studied in terms of the aforementioned characteristics to discuss the possible configurations for the current GPS application.

1.) Orthogonal Mode Dual Frequency Patch Antenna:

As discussed in the cavity model, TM_{01} and TM_{10} modes can be excited on a single rectangular patch to obtain dual frequency operation by adjusting the width and the length of the patch according to the two separate resonant frequencies.

It must be noted that two separate modes are orthogonal that might be a drawback for some applications. However, this behavior makes the configuration a suitable candidate for the GPS applications in which bi-orthogonally polarized dual frequency operation can be achieved by placing two rectangular patches orthogonally.

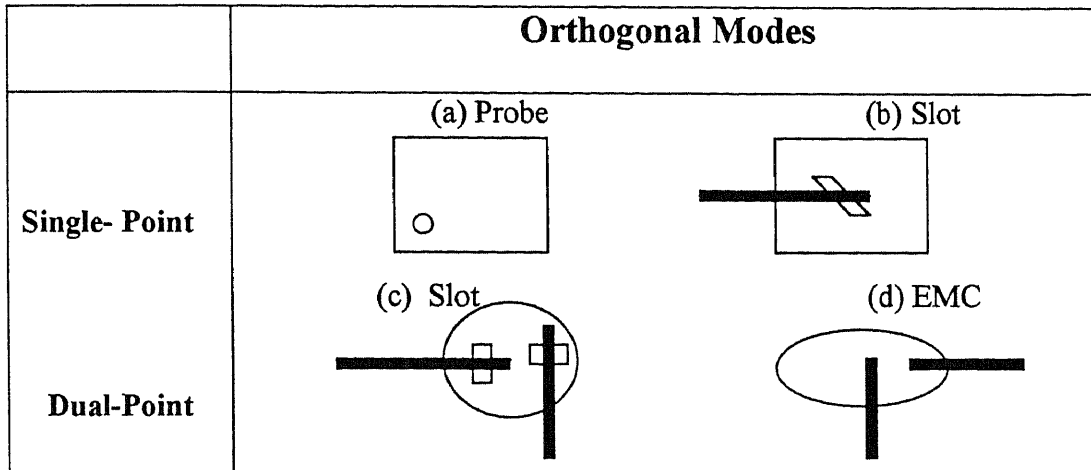


Figure 3.2. Orthogonal-mode dual frequency patch antennas.

As shown in the Figure 3.2, orthogonal modes can be excited either by using a single feed (in the Figure 3.2(a) and 3.2(b)) or by using two separate feeds (in the Figure 3.2(c) and 3.2(d)). As discussed before, the choice depends on the type of application. When separate field configuration is used, as long as the spacing between the feed points is physically realizable, feeds must be positioned close to the center of the corresponding edges in order to obtain good isolation levels between the ports.

The aspect ratio of the rectangular patch is (W_{L1} / W_{L2}) is proportional to the ratio of the frequencies (f_H / f_L) . Therefore orthogonal-mode dual frequency antennas are not suitable for the applications which require large frequency ratios since the H- plane beamwidth at f_H and f_L are determined by W_{L1} and W_{L2} , respectively which results in different radiation characteristics for two separate frequencies. Therefore this discussion also validates the choice of orthogonal mode dual frequency patch antenna configuration for GPS applications, where the frequency ratio is $1.575 / 1.227 = 1.28$.

2.) Multi-patch Dual Frequency Antennas:

The dual frequency behavior is obtained by means of multiple radiating elements, which may be placed in different dielectric layers (stacked), or on the same substrate (coplanar) as shown in the Figure 3.3. In the stacked configuration the length of the corresponding two patches are chosen to obtain resonance at two separate frequencies. Hence, the same configuration can be used to broaden the bandwidth of a single patch antenna by using two stacked patches with close dimensions.

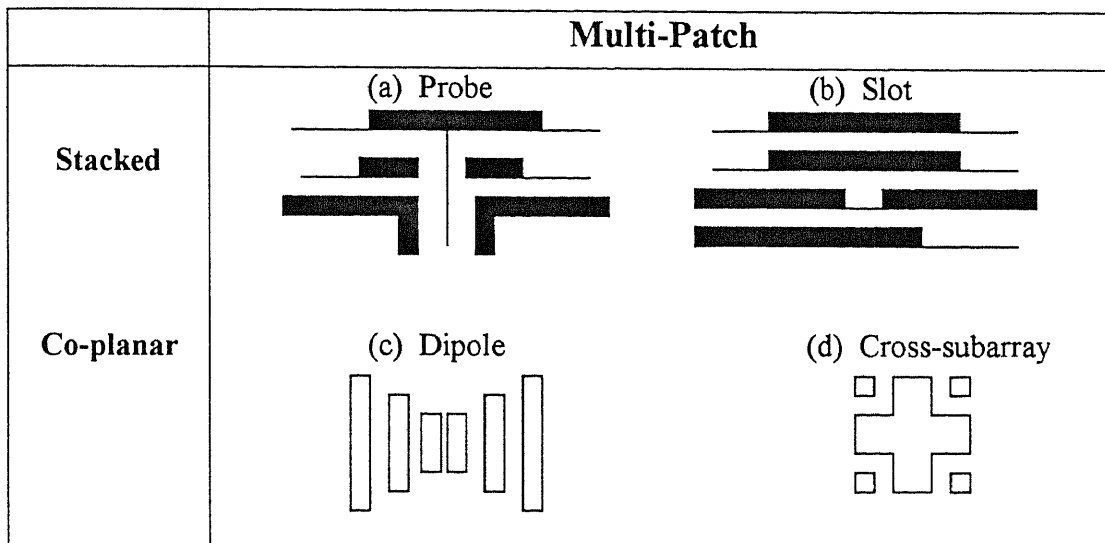
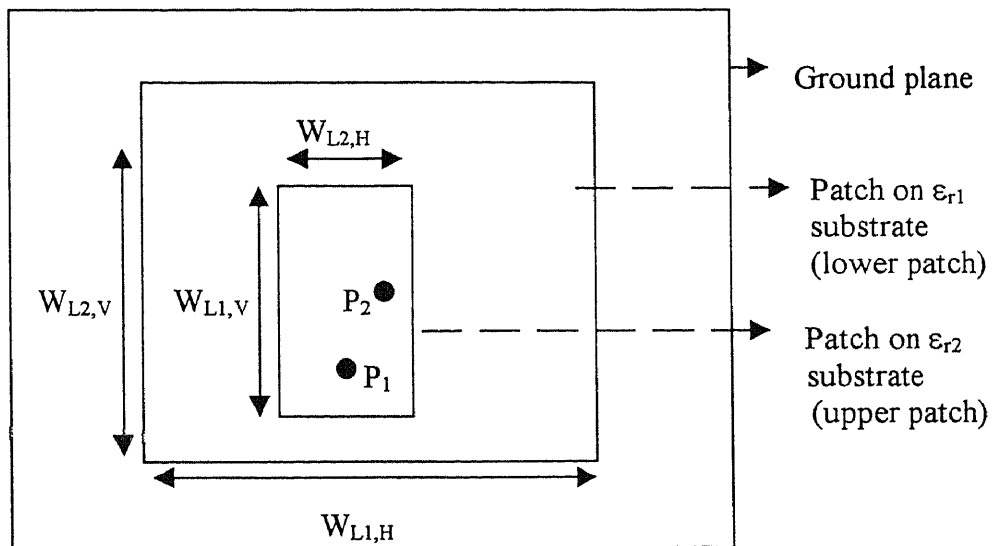


Figure 3.3. Multi-patch dual frequency antennas

Unlike the orthogonal-mode dual frequency patch antennas, these antennas operate with the same polarization at the two frequencies as well as with the dual polarization. However, for the bi-orthogonal dual frequency operation some modifications in the configurations are required. The proposed configuration is shown in the Figure 3.4. For a given set of ϵ_{r1} and ϵ_{r2} , the corresponding lengths ($W_{L1,V}$, $W_{L1,H}$) and ($W_{L2,V}$, $W_{L2,H}$) are designed to be the resonant lengths at f_L and f_H , respectively.

Since the lower patch will behave like a ground plane for the upper one, ϵ_{r2} is chosen to be greater than ϵ_{r1} and the ratio of the cumulative permittivity is adjusted to ensure that the upper patch stays within the limit of the lower one ($W_{L1,V} < W_{L2,V}$). From port one (P_1) vertical polarization at f_L and f_H frequencies will be obtained through the lower and upper patches, respectively. Similarly lower and upper patches will yield the horizontal polarization at f_L and f_H frequencies respectively through port 2 (P_2). The details of the design procedure for the proposed configuration are discussed in Chapter 4.



(a) Top view



(b) Side view

Figure 3.4. Bi-orthogonally polarized dual frequency stacked patch antenna.

Due to the difficulties in optimization of the design, fabrication and tuning of the stacked configuration these types of antennas are not the primary choice in some applications. However, stacked patches provide a better directivity compared to their coplanar counterparts due to increase in the effective aperture of the radiating structure. Hence, for GPS applications, where the gain is an important parameter, stacked patches turn out to be an alternative configuration inspite of the drawbacks during fabrication and tuning phases.

The coplanar dipole configuration with multiple printed resonators as shown in the Figure 3.3.c, is suitable for the applications where more than two resonances are required. In the cross-sub array configuration, as shown in the Figure 3.3.d, the inner crosspatch resonates at one frequency and the outer four square patches resonate at a much higher frequency. Such an antenna configuration becomes useful for the applications that require a large frequency ratio.

3.) Reactively Loaded Patch Antennas:

A microstrip antenna is basically a resonator and by introducing a reactive loading to the patch, a secondary resonance behavior can be obtained. The reactive loading can be achieved by using a coaxial or microstrip line stubs or by inserting notches at the radiating edge of the patch (as shown in Figures 3.5(a)-3.5(d)). However in both cases the frequency ratio cannot be designed to be higher than 1.2 without introducing strong cross-polarization levels or pattern distortion at the additional frequency. To obtain higher values of frequency ratio, the structures shown in the Figures 3.5(f)-3.5(g) can be used in which TM_{10} and TM_{30} modes are excited and the frequency ratio (which is

approximately equal to 3 for the unloaded case) is reduced by loading the antenna with pins, capacitors and /or slots.

TM_{20} mode excitation is not preferred due to the null in the radiation pattern at the broadside direction, therefore, TM_{30} mode is the next mode that can be utilized for the dual-frequency operation. However in this case the frequency ratio is fixed at a large value that is approximately equal to 3. This ratio can be reduced by disturbing the field variations of the TM_{10} and the TM_{30} modes, which are plotted in Figure 3.6 and Figure 3.7, respectively.

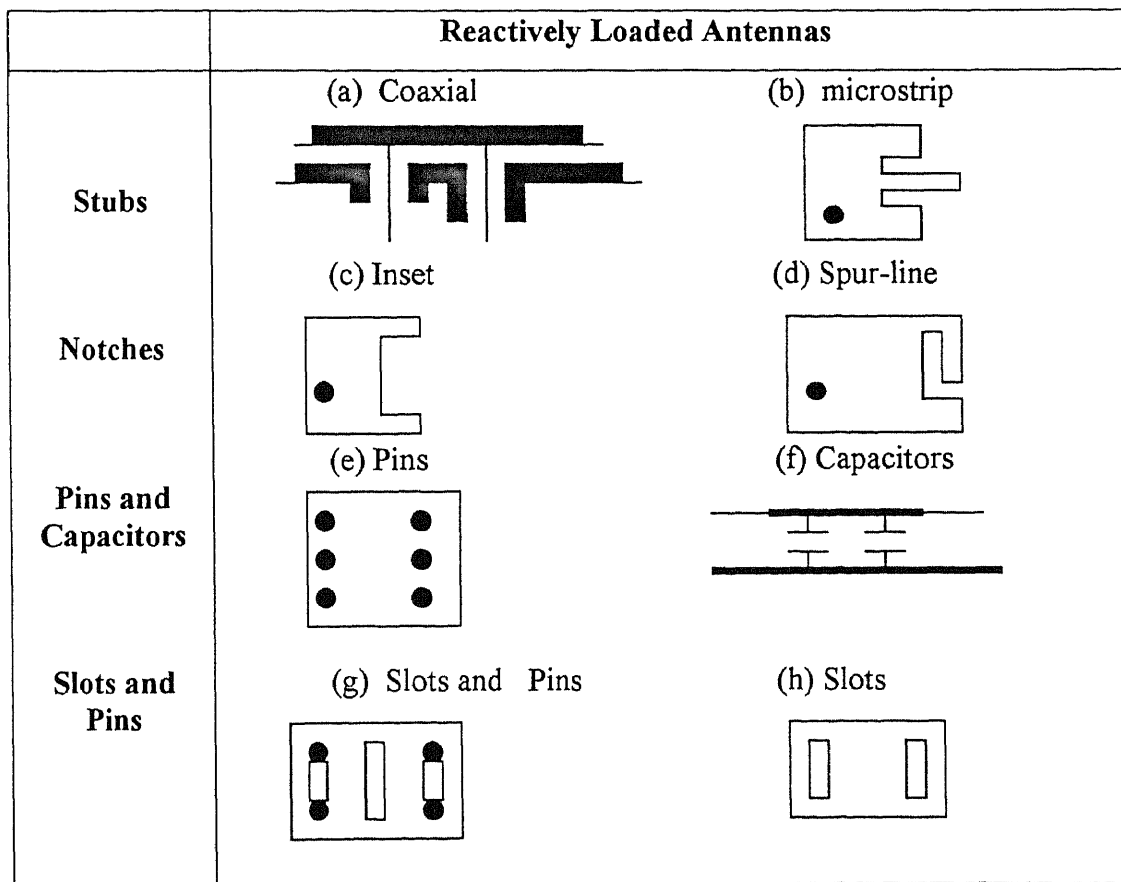


Figure 3.5. Reactively loaded antennas.

As it can be observed from Figure 3.6, by placing shorting pins at a distance $L/6$ from the edges, where the E-field distribution of the TM_{30} mode is zero, the operating frequency of the TM_{10} mode can be increased considerably without affecting the operation of TM_{30} mode. Similarly, slots inserted at the same location as the pins will decrease the resonance frequency of the TM_{30} mode since the H-field distribution of this mode exhibits a maximum at the slot position, see Figure 3.7. By increasing the number of pins and adjusting the length of the slots, the frequency ratio can be

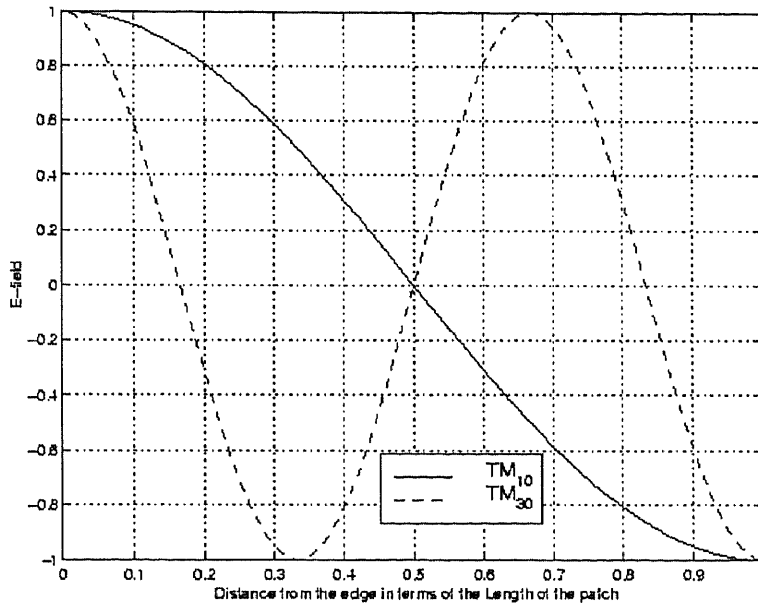


Figure 3.6. Aperture E-field distributions of TM_{10} and TM_{30} modes

lowered from 3 to 1.3. However, the narrower beamwidth and grating lobe characteristics of the radiation pattern at the TM_{30} operating frequency, makes the use of this type of antenna unsuitable in GPS applications which require wide angle coverage ranging from broadside to endfire.

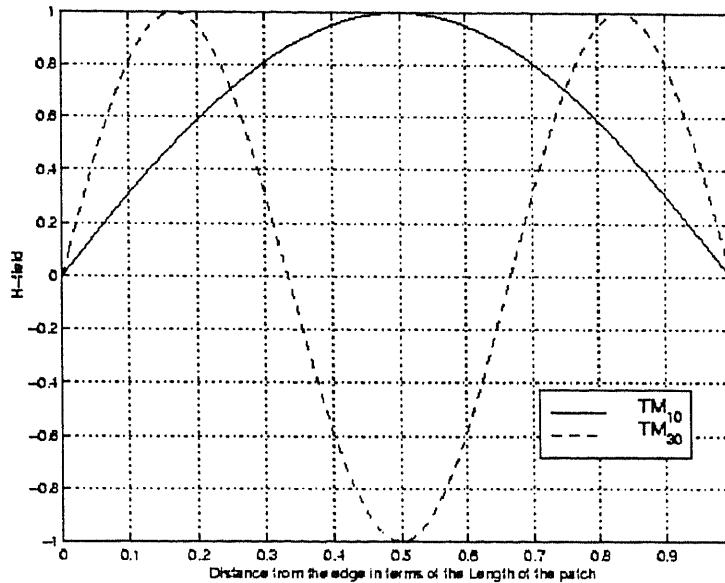


Figure 3.7. Aperture H-field distributions of TM_{10} and TM_{30} modes

Another kind of slot-loaded patch antenna that consists of a rectangular patch with two narrow slots etched close to and parallel to the radiating edge is shown in Figure 3.5.h. In this case also, the dual frequency operation arises from the perturbation of the TM_{10} and the TM_{30} modes. The length of the slots and the dimensions of the patch can be changed to control the frequency ratio in the range from 1.6 to 1.9. However, the length of the slots has a strong effect on the radiation pattern at the higher operation frequency. With shorter slots, radiation pattern is similar to the pattern of the unperturbed TM_{30} mode. As slot length increases, the width of the main beam first reduces and then a null occurs at the broadside. A further increase in the length of the slot will result in a radiation pattern similar to that of the mode. Hence the constraint on the frequency ratio and the irregularities of the radiation pattern eliminates the possibility of utilizing the antenna in GPS applications.

CHAPTER 4

EXPERIMENTAL RESULTS AND DISCUSSIONS

Bi-orthogonally polarized (horizontal and vertical polarization) and dual frequency ($L_1=1.227\text{GHz}$, $L_2=1.575\text{GHz}$) antennas are designed, fabricated, tuned and measured for two different configurations. In Chapter 3, dual frequency printed antenna structures outlined in literature are studied considering GPS application and their performances are compared in terms of impedance matching, gain, radiation efficiency, applicable frequency ratios, ease of fabrication and tuning. It is concluded that coplanar and stacked orthogonal rectangular microstrip patches are the most suitable choices that fulfill the requirements of GPS antenna for the current application. The detailed design procedure and measurement results for these antenna structures are presented below in Section 4.1 and Section 4.2.

4.1 Coplanar Orthogonal Rectangular Dual Patch Antenna

Dual frequency bi-orthogonal operation is achieved through the configuration shown in Figure 4.1, where W_{L1} and W_{L2} denote the resonance lengths at the frequencies L_1 and L_2 , respectively and V and H denotes the vertical and horizontal polarizations, respectively. Feed locations are expressed in terms of the vertical distances from the closest edges (x,y) within the patch antenna.

Considering the overall antenna dimensions being restricted to a maximum dimension of 4.680", a dielectric substrate with a high enough permittivity value that provides a shorter guided wavelength is required. But on the other hand, higher dielectric

values decrease the bandwidth considerably such that a thick dielectric substrate is needed to compensate this limitation by broadening the bandwidth. As a result, an optimum dielectric substrate with a relative dielectric constant of 9.8 and a thickness of 250 mils is chosen to meet the dimension and bandwidth requirements. Availability of the substrate material with a specific relative dielectric constant leads to another constraint hence chosen ϵ_r has to be available commercially.

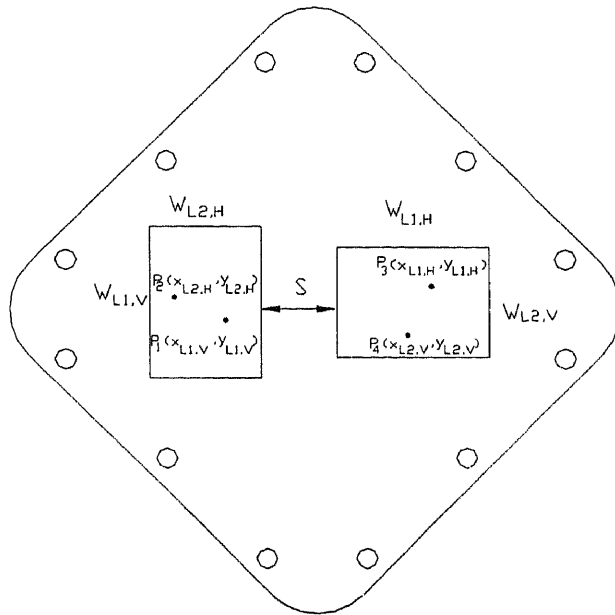


Figure 4.1. Coplanar orthogonal rectangular patches

Transmission line model is used initially to estimate the dimensions of the patch and location of the feed points. The initial estimates are optimized through several iterative simulation steps and final results are obtained by using a full-wave analysis program, IE3D of *Zealand Software Inc.* Good impedance matching (shown in Figure 4.2) and port isolation ($\sim -20\text{dB}$) values are obtained for the following dimensions and feed locations:

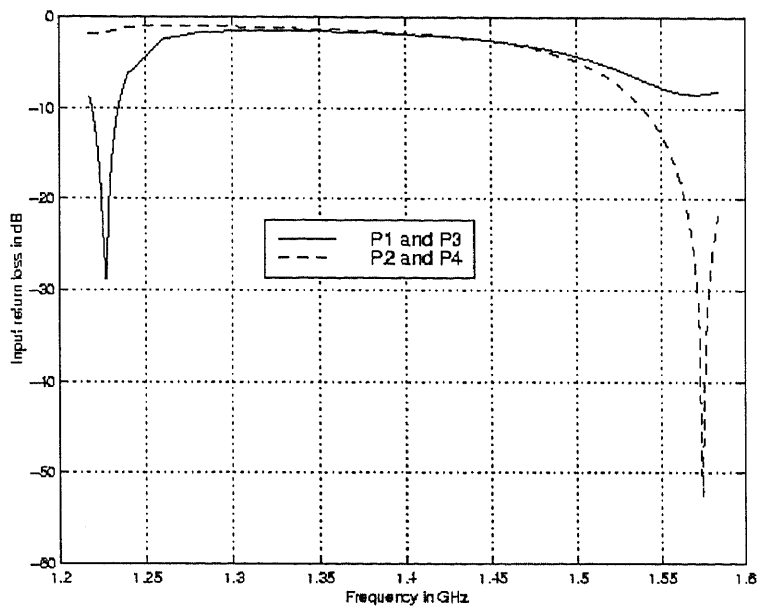


Figure 4.2. Simulation results for the input return loss of the coplanar antenna

The coplanar antenna is fabricated according to these optimized values, and the input return loss and port isolation measurements are carried out using HP 8510C automated vector network analyzer. A shift between the simulated and measured resonance frequency values is observed which may be due to the following effects:

- the full-wave analysis program assumes an infinite ground plane and dielectric substrate model,
- the permittivity of the dielectric substrate may exhibit some variations from its nominal value, due to different batches in manufacturing process,

- the actual size of the patches may not be exactly same as the optimized one due to the limited precision of the etching process.

The dimensions of the patch and feed locations are adjusted with the help of files and adhesive conducting strips in order to tune the antennas to the required operation frequencies. The tuning process is extended to compensate the frequency shifts caused by the cover of the antenna (radome). The Ultra High Molecular Weight Polymer (UHMW) chosen as a radome material, has $\epsilon_r = 2.2$ and loss tangent = 2×10^{-7} at 4 GHz. Simulation results on the effect of relative dielectric constant material as a radome has an effect on overall radiation efficiency of the antenna as shown in Table 1.

Table 1. Radiation efficiency versus ϵ_r of the radome for a single patch of $\epsilon_r = 10$ and thickness $t = 250$ mils

	η - efficiency	
	1.227 GHz	1.575 GHz
No cover	67.34 %	58.23 %
$\epsilon_r = 3.26$	50.8 %	38.93%
$\epsilon_r = 4.85$	47.5%	33.44%

After the tuning is achieved, the dimensions of the antennas and feed locations are measured to be:

$$W_{L1,H} = 1.382''$$

$$W_{L2,H} = 1.007''$$

$$W_{L1,V} = 1.385''$$

$$W_{L2,V} = 1.048''$$

$$(x_{L1,V}, y_{L1,V}) = (0.253'', 0.572'')$$

$$(x_{L1,H}, y_{L1,H}) = (0.472'', 0.300'')$$

$$(x_{L2,V}, y_{L2,V}) = (0.574'', 0.214'')$$

$$(x_{L2,H}, y_{L2,H}) = (0.333'', 0.488'')$$

$$S = 0.940''$$

For each port, the input return loss versus frequency values are measured when the antenna was placed on a 2 square feet ground plane, and graphs are presented in Figure 4.3 and Figure 4.4. The gains of the antennas are measured using commercially available wide-band dual polarized log-periodic antenna, (TECOM, type no. 201085) with an average gain of 7.5dBi within its bandwidth of 1.0 – 4.0 GHz. The relative gain values of the developed antenna are measured as:

$$\text{Gain at 1.227 GHz (vertical polarization)} = 3.62 \text{ dBi}$$

$$\text{Gain at 1.227 GHz (horizontal polarization)} = 3.34 \text{ dBi}$$

$$\text{Gain at 1.575 GHz (vertical polarization)} = 3.36 \text{ dBi}$$

$$\text{Gain at 1.575 GHz (horizontal polarization)} = 2.73 \text{ dBi}$$

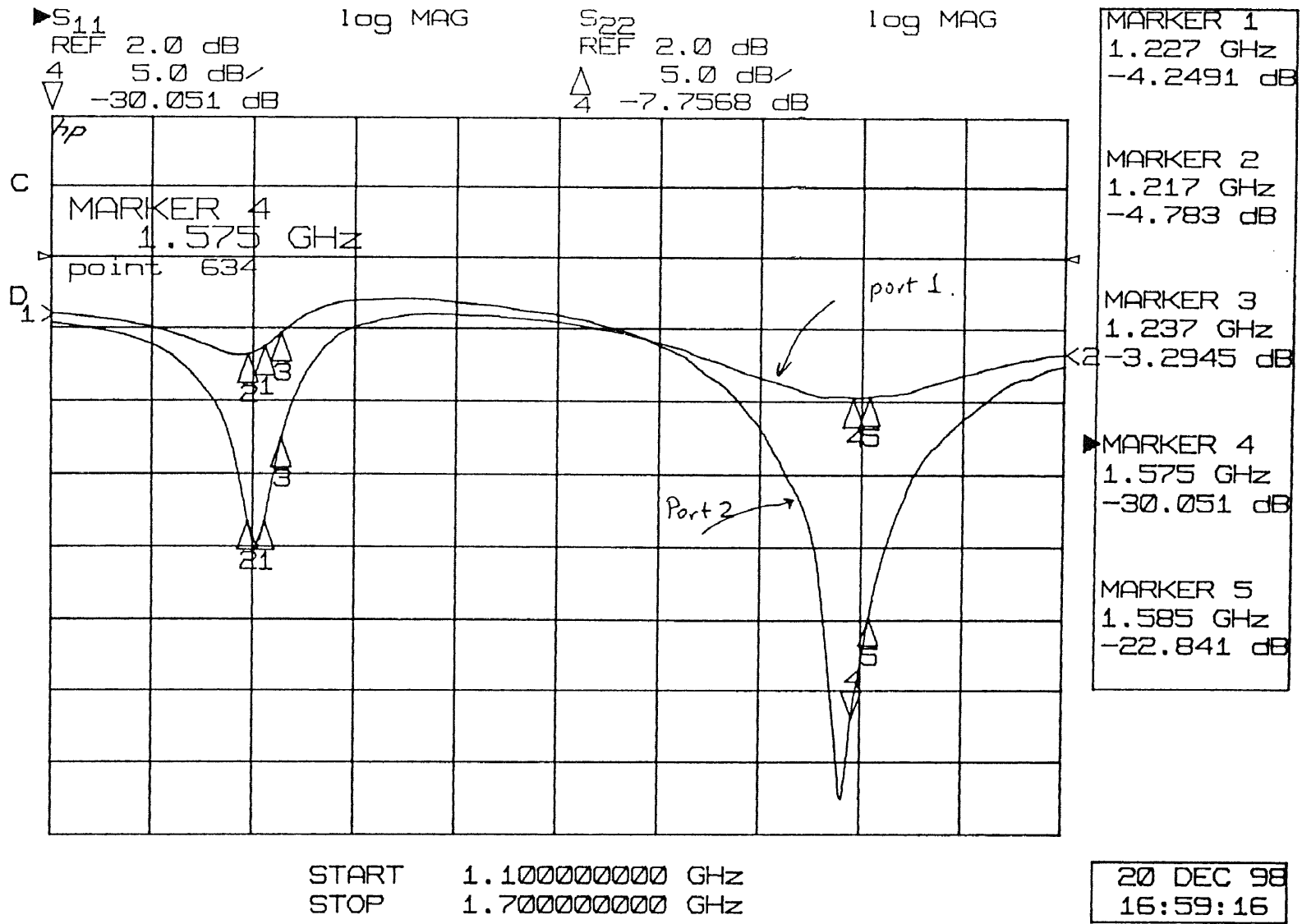


Figure 4.3. Measured input return loss graph for port 1 and port 2

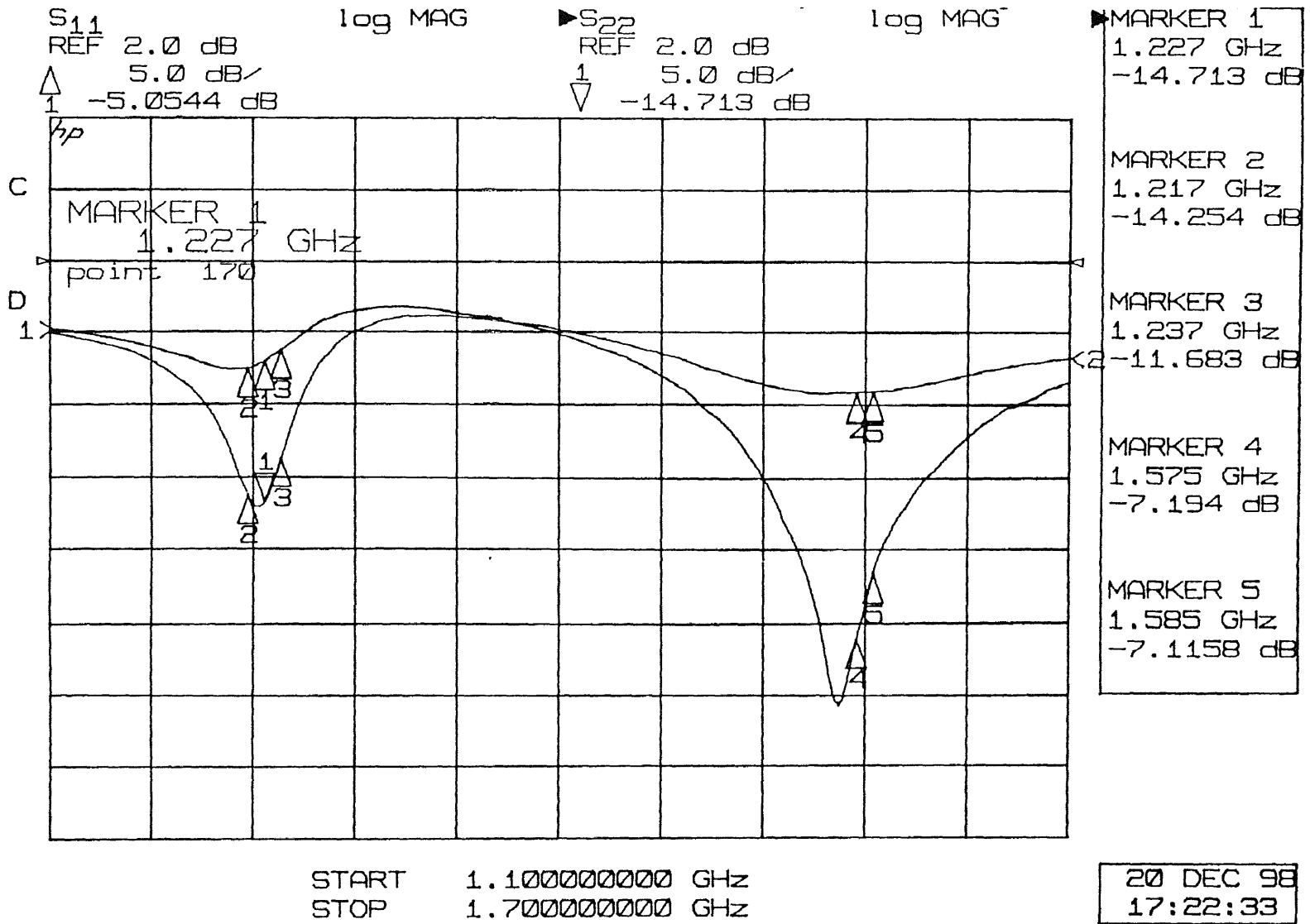


Figure 4.4. Measured input return loss graph for port 3 and port 4

Finally, the radiation patterns of the antennas are measured in two principle planes (E and H planes) and they are plotted in Figure 4.5 – Figure 4.8.

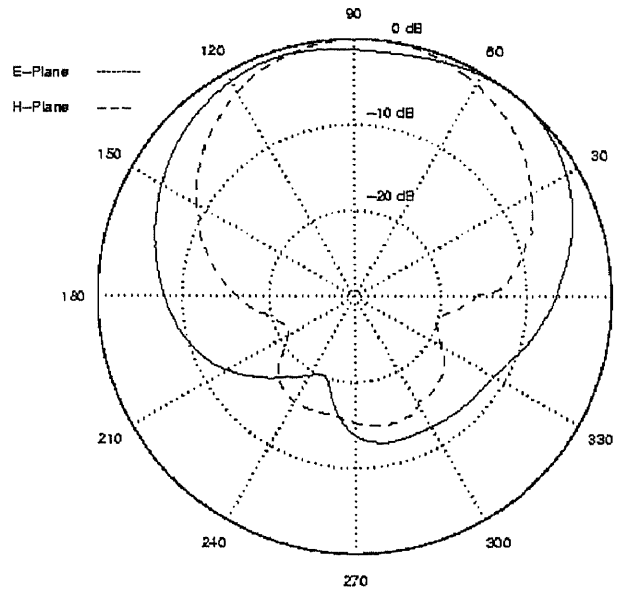


Figure 4.5. Radiation patterns at 1.227 GHz for vertical polarization

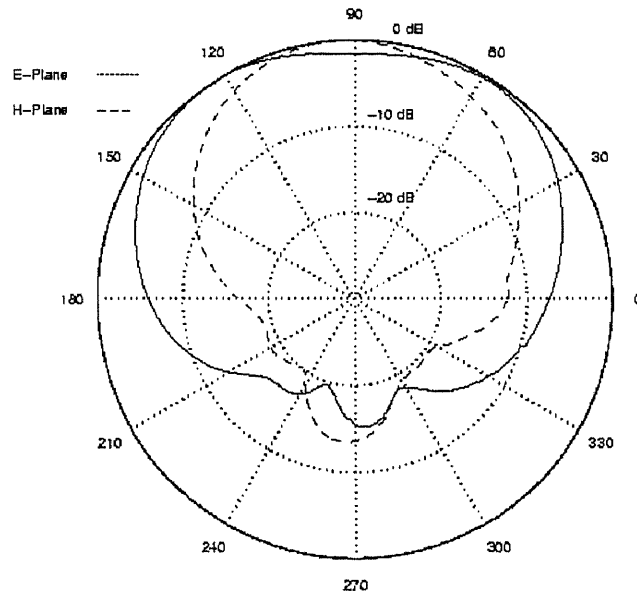


Figure 4.6. Radiation patterns at 1.227 GHz for horizontal polarization

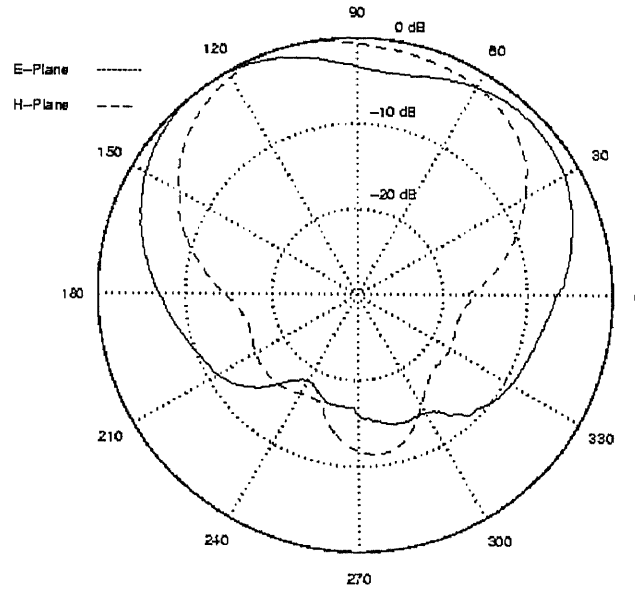


Figure 4.7. Radiation patterns at 1.575 GHz for vertical polarization

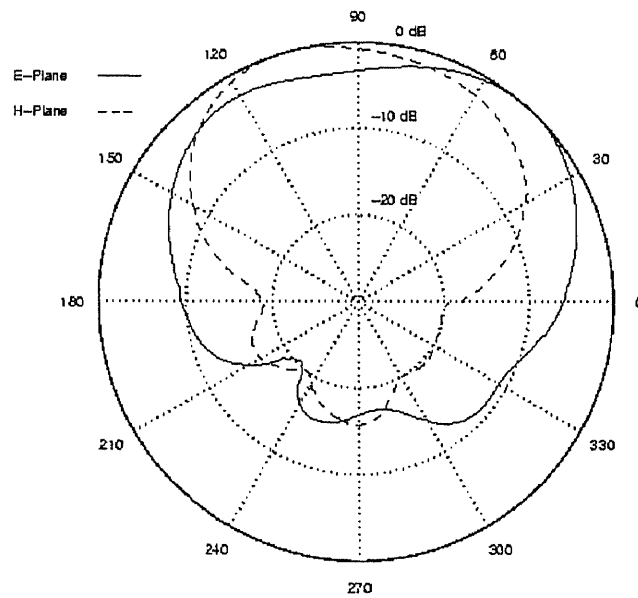


Figure 4.8. Radiation patterns at 1.575 GHz for horizontal polarization

Some dips are observed in the radiation patterns and measurements are repeated for several low loss antenna covers with different tapering levels to test the effect of radome on the radiation pattern. However an improvement in the dips could not be obtained. The thick and high permittivity dielectric substrate is prone to excite surface waves, which may cause the degradation of the radiation patterns. Comparing the radiation patterns at different frequencies it can be observed that the dips are more dominant at the higher operation frequency of 1.575 GHz. This observation support the hypothesis on attributing the cause of dips to the surface wave excitation since the contribution of the surface wave poles are stronger at higher frequencies.

4.2 Stacked Orthogonally Polarized Rectangular Patch Antennas

The stacked orthogonal patch antenna configuration designed to obtain bi-orthogonal dual frequency operation is shown in Figure 4.9.

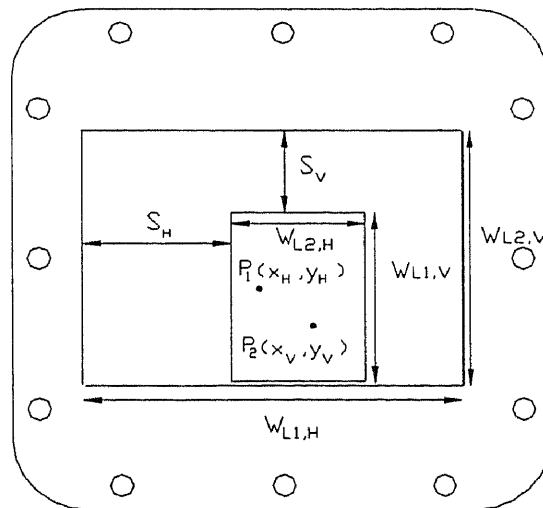


Figure 4.9. Stacked orthogonal rectangular patch antennas

Horizontal polarization at L_1 and L_2 frequencies are obtained through port 1 from the lower and upper patches, respectively. Similarly, vertical polarization at L_1 and L_2 frequencies are obtained through port 2 from the upper and lower patches, respectively. When the upper patch is centered with respect to the lower one, the feed positions can not be adjusted with respect to each patch independently. Hence, the offset values S_H and S_V are introduced to be able to match the ports at these two operation frequencies. Feed locations and offset values are given by considering the lower left corner of the lower patch as the origin.

Due to the advantage of the stacked configuration, the available larger area permits the use of a dielectric substrate with a lower permittivity value. Thus a dielectric substrate with a relative permittivity of 2.2 and thickness of 120 mils is used for the lower layer. In order to restrict the dimensions of the upper patch within the lower one, a high dielectric constant ratio is required, therefore, a dielectric substrate with a relative permittivity of 9.8 and thickness of 125 mils is chosen for the upper layer.

Using the IE3D software the stacked structure is simulated, the dimensions and feed positions are optimized to the following values to obtain good input impedance matching values as shown in Figure 4.10. The isolation between the ports is in the order of -10dB at the operation frequencies.

$$W_{L1,H} = 2.7165''$$

$$W_{L2,H} = 1.1417''$$

$$W_{L1,V} = 1.5354''$$

$$W_{L2,V} = 2.047''$$

$$(x_V, y_V) = (1.4337'', 0.5511'')$$

$$(x_H, y_H) = (0.9842'', 0.8464'')$$

$$S_V = 0.0393''$$

$$S_H = 0.7480''$$

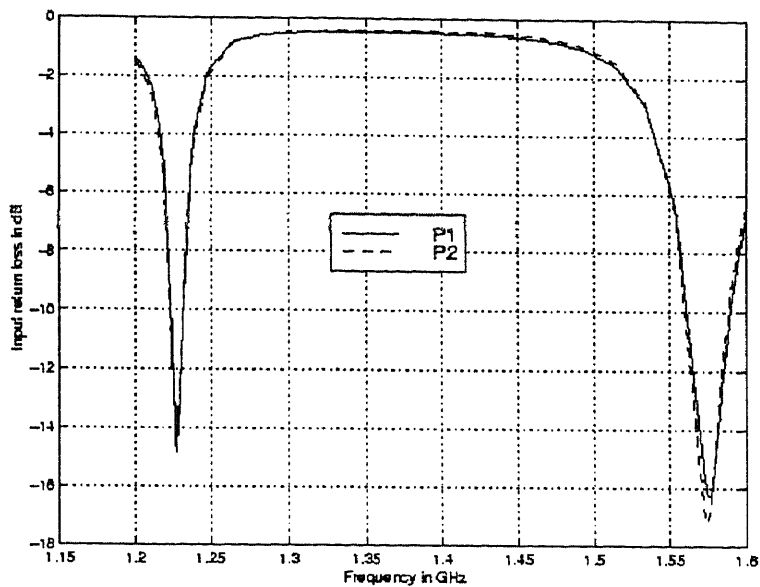


Figure 4.10. Simulation results for the input return loss of the stacked antenna

The stacked antenna is fabricated, tuned and measured. Compared to the coplanar antenna, a larger shift between the simulated and measured resonance frequencies is observed. This behavior may be associated with the numerical modeling of the more complex feeding structure used for the stacked configuration. In addition to adjusting the patch dimensions and feed locations, the size of the hole in the coupled lower patch is used as a variable and helped to improve tuning. After tuning the dimensions are measured as:

$$W_{L1,H} = 2.8212''$$

$$W_{L2,H} = 1.3572''$$

$$W_{L1,V} = 1.898''$$

$$W_{L2,V} = 2.1255''$$

$$(x_V, y_V) = (1.4662'', 0.555'')$$

$$(x_H, y_H) = (1.8967'', 0.8710'')$$

$$S_V = 0.0415''$$

$$S_H = 0.8037''$$

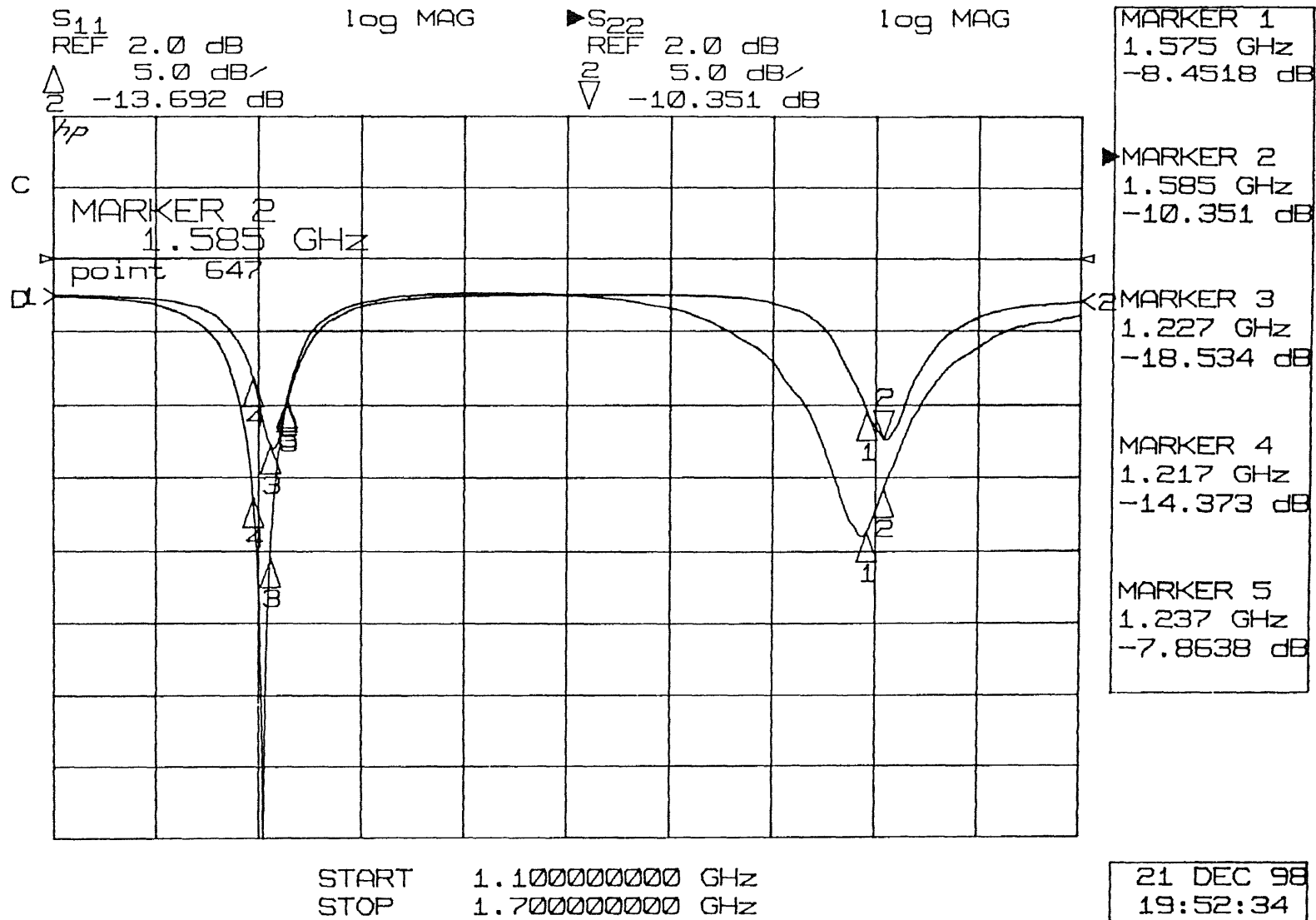


Figure 4.11. Measured input return loss graph for port 1 and port 2

The input return loss values are measured after tuning the antenna and the results are plotted in Figure 4.11. It can be observed that a good matching characteristic as in the coplanar configuration could not be obtained through the stacked structure. In spite of this increase in the input return loss, the measurement results listed below shows that the stacked configuration exhibits gain values as high as the coplanar one. It might be that the loss due to the mismatch is compensated by the higher directivity, which is a result of larger effective aperture obtained through the stacked configuration.

Gain at 1.227 GHz (vertical polarization) = 3.8 dBi

Gain at 1.227 GHz (horizontal polarization) = 3.09 dBi

Gain at 1.575 GHz (vertical polarization) = 2.81 dBi

Gain at 1.575 GHz (horizontal polarization) = 2.73 dBi

Finally, the radiation patterns of the stacked antenna are measured in two principle planes (E and H planes) and they are plotted in Figure 4.12 – Figure 4.15.

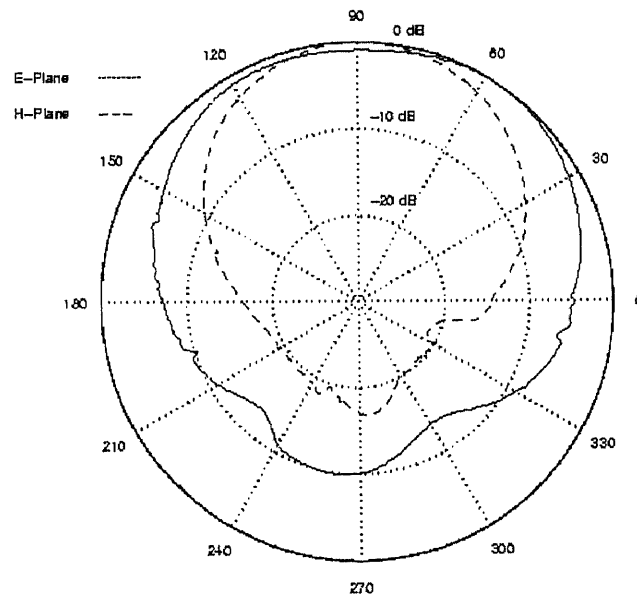


Figure 4.12. Radiation patterns at 1.227 GHz for vertical polarization

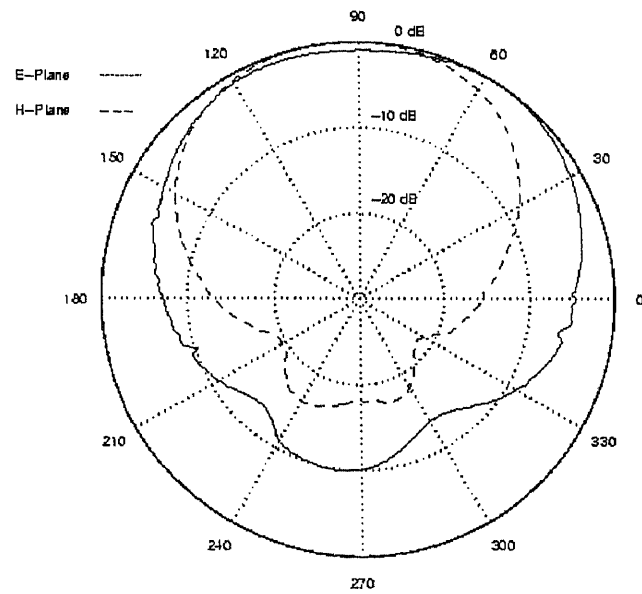


Figure 4.13. Radiation patterns at 1.227 GHz for horizontal polarization

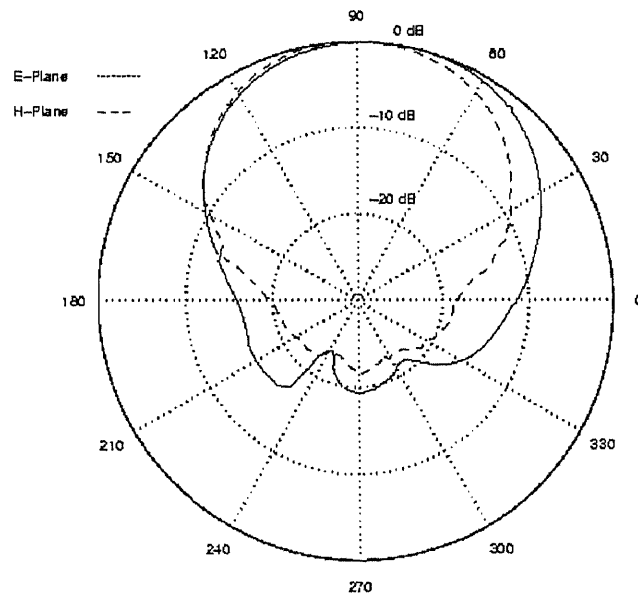


Figure 4.14. Radiation patterns at 1.575 GHz for vertical polarization

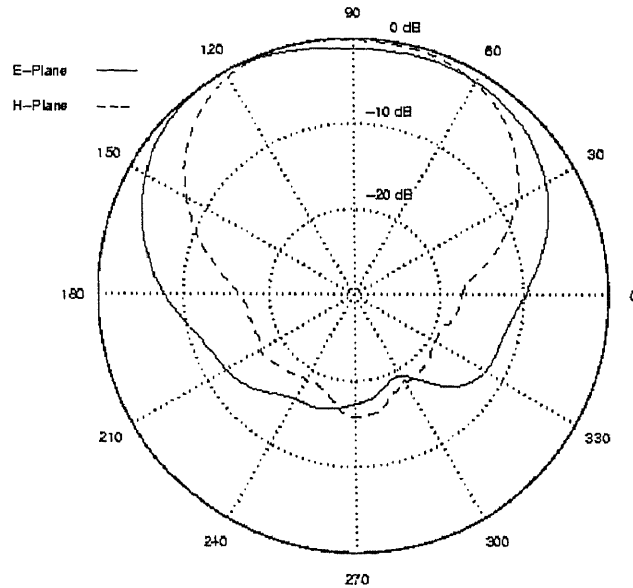


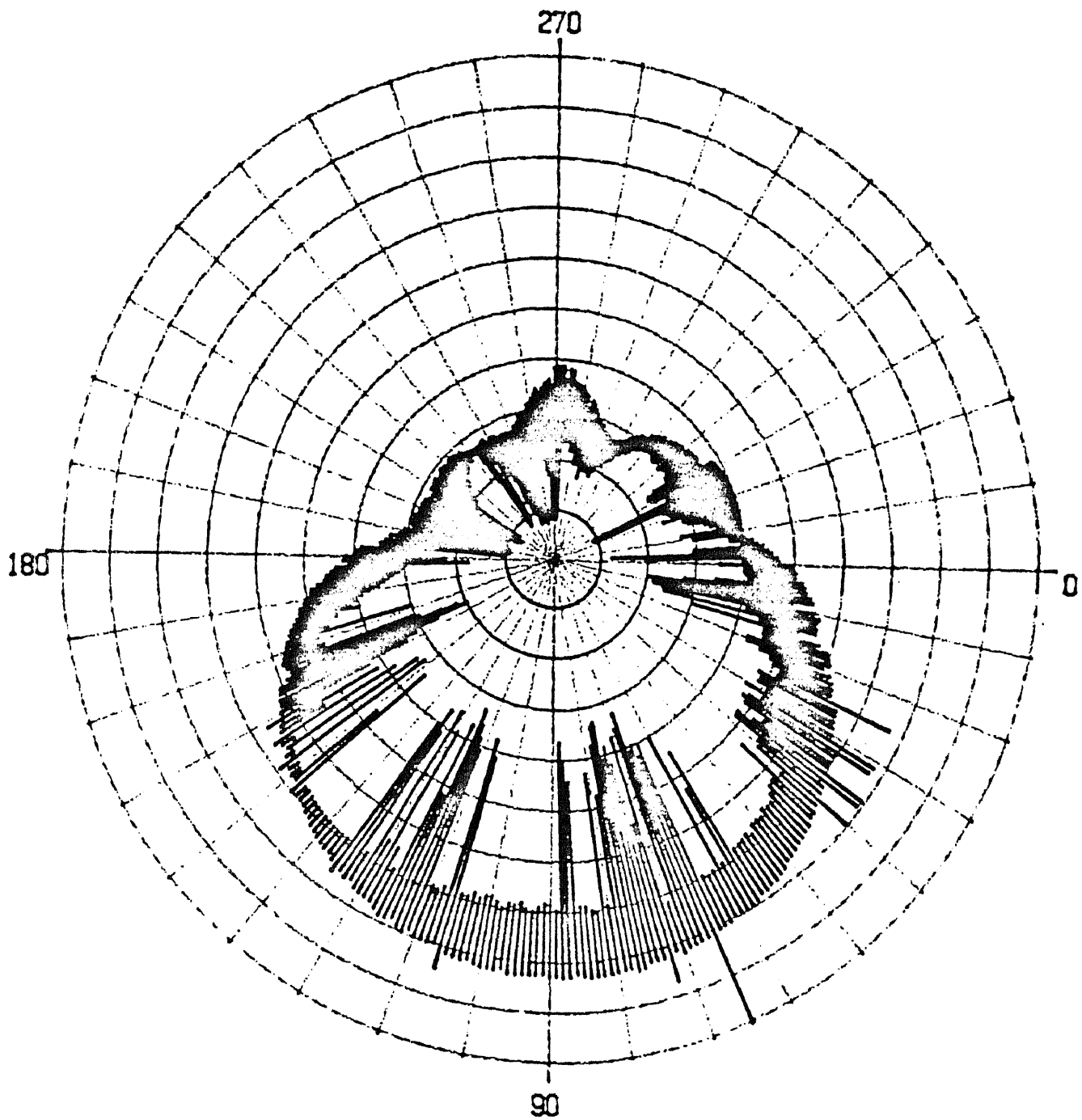
Figure 4.15. Radiation patterns at 1.575 GHz for horizontal polarization

Comparing the radiation pattern plots of the stacked and coplanar antennas, it is observed that the dips that occur in the coplanar configuration disappear in the stacked one. Note that the surface waves that might be the cause of the distortions in the radiation patterns may not be supported in the stacked structure as thinner dielectric substrates are used. Design and fabrication of the stacked configuration with relative dielectric constants of $\epsilon_r=2.20$ and 9.8 , but with thickness of 250 mils for each layer is in progress. It is expected that thicker substrates will result in increased bandwidths for both L1 and L2 bands.

Polarization measurements:

Polarization measurements of the antennas developed in this work have been carried out using the set-up where linearly polarized antenna used for receiving purposes was rotated

a Circular Polarization (CP) mode using a hybrid coupler is shown in Figure 4.16, where this antenna was used for transmission. The axial ratio was measured. The set has to be fine tuned for further accuracy in determining the range of angles for which the antenna operates in a CP mode.



Scale Step -4 dBm Whole Scale 40 dBm Max Power = -17.33 dBm

Frequency is 1.575 GHz Power level is 15 dB

Figure 4.16. Polarization Pattern of the stacked antenna connected to a hybrid coupler at 1.575 GHz.

CHAPTER 5

CONCLUSIONS

Dual frequency bi-orthogonally polarized antennas to be used in Global Positioning System applications operating in L1 (1575.42 ± 10.23 MHz) and L2 (1227.60 ± 10.23 MHz) bands has been designed using CAD tools, the optimized design values served as a guide for fabrication. Final tuning has been carried out to meet the strict requirements needed for file operations. The antenna dimensions were limited to 4.120" x 4.680" x 1.250" dimensions including the radome. Orthogonally placed two dual frequency probe excited patches were designed using high dielectric constant substrate ($\epsilon_r = 9.8$ and thickness of 250 mils, Rogers TMM10i material) to obtain vertical and horizontal polarization for each band. The measured performance of this antenna showed good agreement with the specifications required to meet the application needs. As an alternative, a stacked dual patch antenna configuration was also considered and a prototype antenna has been developed. Using low and high dielectric constants of 2.20 and 9.8 and relative thickness of 125 mils for each layer an orthogonally placed dual patch configuration has been designed, fabricated and tested. Effects of radome using materials with different permittivities have been studied through numerical simulations in terms of radiation efficiency and radomes have been fabricated using various materials including UMHW, HDPE and Delrin. Numerical simulations have been carried out using IE3D software package developed by Zealand Software Inc. Antennas that were fabricated based on optimized parameters have further required tuning due to inaccuracies in simulation and material properties. The measurement setup has been

enhanced to accommodate axial ratio measurements in polarization pattern characterized by adding rotary joint to rotate linearly polarized antenna operating in the receiving mode. The performance characteristics showed that adequate bandwidths and beamwidths were obtained and gain of these antennas were measured to be in the order of 3.5 dBi along the main lobe. Further work is continuing to obtain antennas with wider bandwidths using thicker substrates.

APPENDIX

ELECTROMAGNETIC SIMULATION SOFTWARE

Currently available various commercial electromagnetic simulation software packages are based on numerical methods such as:

- Method of Moments (MoM) in Spectral Domain,
- Method of Moments in Spatial Domain,
- Finite Element Method (FEM),
- Finite Difference Time Domain Method (FDTD) [5], and Transmission Line Matrix Methods (TLM) [6].

Each method has its own advantages as well as disadvantages depending on the particular specifics of the given application. The brief description of each method and its relation to the work done in this thesis are presented below:

1.) Method of Moments in Spectral Domain: This method has been developed for analysis of structures commonly described as closed problems, i.e. filters, resonators, etc. The antenna problem considered in this work falls into a class commonly described as an open problem requiring the usage of radiation condition. Due to limitation of the spectral domain approach, boundary conditions which require usage of radiation condition are not adequately addressed by this method. Additional inherent disadvantage is due to uniform sampling required through usage of FFT built into this method. Closed structures such as hybrid ring couplers will be modeled inaccurately due to inadequate a spect of the uniform sampling.

2.) ***Finite Element Method:*** The main disadvantages of this method is that it requires exhaustive computational effort (number crunching) as well as extensive RAM requirements. As a result, it takes a long time to compute structures of even moderate size. However it does not encounter limitation in terms of geometrical shape constraints. In the future when computer speed and RAM will not be of a concern, then FEM may become an attractive method for electromagnetic simulation. Recent efforts in extending FEM into time domain may lead to a new possibility if the above mentioned difficulties are alleviated.

3.) ***Finite Difference Time Domain (FDTD) and Transmission Line Matrix (TLM) methods :*** Both methods have similar difficulties. They require solution of both magnetic and electric fields in three dimensional space, therefore, the number of unknown variables increase significantly. They need uniform gridding, extensive computer power and memory, and therefore it takes a long time to complete the desired simulation. The most outstanding features of both methods is that they are simple to be programmed and they produce results in time domain directly. It needs only one execution in time which can offer a corresponding wideband frequency response. Additional attractiveness in FDTD is its usage in conjunction with circuit simulators, since it has the ability to handle lumped components effectively.

4.) ***Method of Moments in Spatial Domain Method:*** It is an open boundary simulator. It uses both rectangular and triangular cells, therefore, it has a capability to simulate arbitrary shapes. The main attractive feature of this approach is that it requires

solution of the current distribution on the conductors only in the 3-D, multi-layered sections, therefore it takes a lot less time than FEM, FDTD, & TLM. Therefore, it is the most suitable software due to its capabilities and its efficiency to be used in the current application with available limited computer resources.

IE3D (Integrated Equation Solution 3D)

The emerging electromagnetic simulation tools in microwave/millimeter-waves engineering are forming backbone for the successful fabrication of complicated high density circuits built as microwave monolithic integrated circuits (MMIC) chips for applications in transmitters, receivers, amplifiers, phase detectors, etc.

The three most basic transmission lines employed in the MMIC technology are microstrip, slotted-line, and co-planar waveguides, which all can be classified as planar structures. In the past, the dominant transmission guides were either heavy and bulky rectangular, cylindrical hollow metallic waveguides or coaxial cables. Unlike conventional classical waveguide structures, exact analytical analysis of open guided quasi-TEM mode and higher order modes are not available, therefore numerical analysis is the only means in attempting to solve these complicated issues.

IE3D [6] is based upon a full-wave integral equation, solved by method of moments. Current distributions on a true 3-D, multi-layered metallic structures of arbitrary shapes are determined as an outcome of these simulations. In the IE3D software tool, currents on true 3-D metalization can be modeled at any arbitrary angle. It automatically discretizes regular region with rectangular cells and irregular region with triangular cells. Rectangular cells yield faster solutions whereas triangular cells require

longer computational time. With this automatic mixed meshing rectangular and triangular cells capability, IE3D provides nearly optimum solutions for arbitrary shape structures.

IE3D has a total of three modules: MGRID, MODUA, and CURVIEW. MGRID is a Windows 95 or Windows NT graphical layout editor. MODUA is a post-processor for calculating S-parameters and impedance. CURVIEW is also a post-processing tool capable of determining current distributions, current distribution vectors, and 3-D radiation patterns.

One of the best features of the IE3D is its built-in gradient optimization routine which is especially valuable in this application in determining the resonant length of the patch, as well as the location of the feed probe. Because the location of the probe has an effect on both input impedance and resonant frequency of the antenna, it is very difficult simultaneously to place the probe where one can match the antenna and also optimize the antenna size for the desired resonant frequency. With such built-in optimization in IE3D, the user can optimize simultaneously the optimum feed point location as well as the desired resonant frequency dimension. Scalar and vector current distributions are also very important features which help the user to be able to visualize where current heavily concentrates and in which direction the current flows in the given geometry. True 3-D radiation pattern, mapped 3-D radiation patterns, polar and rectangular display of 2-D patterns, gain, directivity, all are evaluated and are provided as output parameters. All these features are very practical as trouble shooting tools for the analysis and design of general radiating structures.

REFERENCES

- [1] Murray W. Rosen and Michael S. Braasch, "Low-Cost GPS Interference Mitigation Using Single Aperture Cancellation Techniques", Navigation 2000-1998 ION National Technical Meeting, The Institute of Navigation, Long Beach, CA, January 1998.
- [2] Robert E. Munson, "Microstrip Antennas", *Antenna Engineering Handbook*, edited by Richard C. Johnson and Henry Jask, Chapter 7, Long Island, New York, McGraw Hill, 1984.
- [3] S. Maci and G. Biffi Gentili, "Dual Frequency Patch Antennas", *IEEE Antennas and Propagation Magazine*, Vol. 39, No 6, December 1997.
- [4] Balanis, Constantine A., *Antenna Theory Analysis & Design*, New York, NY, John Wiley & Sons Inc., 1997.
- [5] Christopoulos, Christos, *The Transmission-Line Modeling Method TLM*, The IEEE PRESS, 1995.
- [6] Bahl, I.J., and Trivedi, D.K., "A Designer's guide to microstrip line," *Microwaves*, May 1997.
- [7] Cohn, S., "Characteristic impedance of the shielded-strip transmission line," *IRE Trans. Microwave Theory and Techniques*, Vol. MMT-2, No. 7, p.52, July 1954.
- [8] Hammerstad, E.O., "Equation for Microstrip Circuit Design," *Proc. Fifth European Microwave Conf.*, pp. 268-272, Sept. 1975.
- [9] David M. Pozar and Daniell H. Schaubert, *Microstrip Antennas, The Analysis and Design of Microstrip Antenna and Arrays*, New York, IEEE Press.
- [10] Derneryd, A., "A Theoretical Investigation of the Rectangular Microstrip Antenna Elements," *IEEE Tran. On Antenna and Propagation*, Vol. AP-26, pp 523-535, 1978.
- [11] Lo, Y.T., Solomon, D. and Richards, W.F., "Theory and Experiment on Microstrip Antenna," *IEEE AP-S Symposium (Japan)*, pp. 53-55, 1978.